A chronostratigraphic framework for the upper Stormberg Group: implications for the Triassic-Jurassic boundary in southern Africa

– TJB special volume in Earth-Science Reviews –

Emese M. Bordy[1,*], Miengah Abrahams[1], Glenn R. Sharman[2], Pia A. Viglietti[3,4,5], Roger B. J. Benson[3,6], Blair W. McPhee[3], Paul M. Barrett[3,7], Lara Sciscio[1,8], Daniel Condon[9], Roland Mundil[10], Zandri Rademan[11], Zubair Jinnah[5], James M. Clark[12], Celina A. Suarez[2], Kimberley E. J. Chapelle[3,5], Jonah N. Choiniere[3]

1 Department of Geological Sciences, University of Cape Town, Private Bag X3, Rondebosch 7701, South Africa.
2 Department of Geosciences, University of Arkansas, 340 N, Campus Drive, Fayetteville, Arkansas, 72701, United States.
3 Evolutionary Studies Institute, University of the Witwatersrand, Johannesburg, Private Bag 3 Wits 2050, South Africa.
4 Integrative Research Center, Field Museum of Natural History, 1400 South Lake Shore Drive, Chicago, IL, 60605, United States.
5 School of Geosciences, University of the Witwatersrand, Johannesburg, Private Bag 3, Wits 2050, South Africa.
6 Department of Earth Sciences, University of Oxford, Oxford, OX1 3AN, United Kingdom.
7 Department of Earth Sciences, Natural History Museum, Cromwell Road, London, SW7 5BD, United Kingdom.
8 Department of Geology, University of Johannesburg, Kingsway and Auckland Park, 2006 Johannesburg, South Africa.
9 British Geological Survey (BGS), Keyworth, Nottingham, NG12 5GG, United Kingdom.
10 Berkeley Geochronology Center (BGC), 2455 Ridge Road, Berkeley, California 94709, United States.
11 Department of Earth Science, Stellenbosch University, Private Bag X1, Matieland, 7602, South Africa.
12 Department of Biological Sciences, The George Washington University, 800 22nd St. NW Suite 6000, Washington, D.C. 20052, United States.

* - Corresponding author: emese.bordy@uct.ac.za

Abstract

The upper Stormberg Group (Elliot and Clarens formations) of the main Karoo Basin is well-known for its fossil vertebrate fauna, comprising early branching members of lineages including mammals, dinosaurs, and testudinates. Despite 150 years of scientific study, the upper Stormberg Group lacks radioisotopic age constraints and remains coarsely dated via imprecise faunal correlations. Here we synthesise previous litho- and magnetostratigraphic studies, and present a comprehensive biostratigraphic review of upper Stormberg fauna. We also present the results of the first geochronological assessment of the unit across the basin, using U-Pb dates derived from detrital zircons obtained from tuffaceous sandstones and siltstones, the youngest of which are considered maximum depositional ages. Our results confirm that the Elliot Formation contains the Triassic–Jurassic boundary, making it one of the few fossiliferous continental units that records the effects of the end-Triassic Mass Extinction event. Our work suggests a mid-Norian–Rhaetian age for the lower Elliot Formation and a Hettangian–Sinemurian age for the upper Elliot Formation, although the precise stratigraphic position of the Triassic/Jurassic (Rhaetian/Hettangian) boundary remains somewhat uncertain. A mainly Pliensbachian age is obtained for the Clarens Formation. The new dates allow direct comparison with better-calibrated Triassic-Jurassic faunas of the Western Hemisphere (e.g., Chinle and Los Colorados formations). We show that sauropodomorph, but not ornithischian or theropod, dinosaurs were well-established in the main Karoo Basin ~220 million years ago, and that typical Norian faunas (e.g., aetosaurs, phytosaurs) are either rare or absent in the lower Elliot Formation, which is paucispecific compared to the upper Elliot. While this is unlikely the result of geographic sampling biases, it could be from historical sampling intensity differences.

Keywords: U–Pb detrital zircon geochronology; main Karoo Basin; Elliot Formation; vertebrate biostratigraphy; early dinosaurs; magnetostratigraphy

Motto:

"Africa presents incomparable opportunities for geological studies; the area is vast; the workers are comparatively few. The time has not yet arrived for extremely detailed studies […] Consequently, a temptation to generalize is ever present; and it is certain that conclusions reached by workers of my and preceding generations will demand constant revision in the light of new knowledge." Sidney Henry Haughton (1888—1982) [in Dunham, K.C., 1983. Sidney Henry Haughton, 7 May 1888—24 May 1982. https://doi.org/10.1098/rsbm.1983.0011]

1. Introduction

The Upper Triassic to Lower Jurassic upper Stormberg Group (Elliot and Clarens formations) in the main Karoo Basin (MKB) of southern Africa (Fig. 1) is rich in both vertebrate body and trace fossils and serves as a global standard for Triassic-Jurassic boundary (TJB) studies. This fossil record is critical for understanding Early Mesozoic terrestrial vertebrate evolution, and it includes remains of dinosaurs, pseudosuchians, lepidosaurs, stem-group turtles, temnospondyl amphibians, and later-branching therapsids, as well as their tracks and trackways (e.g., Ellenberger et al., 1964; Ellenberger, 1970, 1972, 1974; Kitching and Raath, 1984; Knoll, 2004, 2005). Faunal and sedimentary facies changes informally divide the Elliot Formation (EF) into lower (lEF) and upper (uEF) sections (e.g., Ellenberger et al., 1964; Kitching and Raath, 1984; Bordy et al., 2004 a, b, c, d). Historically, the lEF and uEF were both considered to be Upper Triassic (e.g., Haughton, 1924), but more recent work based on intercontinental faunal correlations has proposed that they represent Late Triassic and Early Jurassic depositional ages, respectively (e.g., Olsen and Galton, 1984; Lucas and Hancox, 2001). If these correlations are correct, then the Elliot Formation is indeed one of the few fossiliferous continental deposits that spans the end-Triassic Mass Extinction event (ETME). This makes it crucially important for understanding shifts in the terrestrial ecosystems of southern Pangaea through the TJB interval. However, these age assessments have not been tested using geochronological methods and, instead, rely on low-precision ichno- and biostratigraphic correlations. This prevents the rich fossil record of the Elliot Formation from being fully used for studying the dynamics of extinction and recovery during the ETME.

Determining the depositional age of clastic sedimentary rocks is challenging, particularly in the absence of widespread and age-specific fossils or interbedded geochronologically datable primary volcanic tuff layers - the products of co-genetic volcanic events. Within the Karoo Supergroup in the main Karoo Basin (Figs. 1, 2), the Permo-Triassic Beaufort Group is a leading example of a

radioisotopically well-dated, highly fossiliferous stratigraphic unit (e.g., Rubidge et al., 2013; Viglietti et al., 2018a). In contrast, radioisotopic dates have not been used to constrain stratigraphic hypotheses for the overlying Stormberg Group, which encompasses the Molteno, Elliot and Clarens formations. Although both groups are globally recognised for their rich continental fossil assemblages and associated record of mass extinctions, the lack of a high-resolution chronology in the Stormberg Group limits its biostratigraphic utility. One reason for this is that the Stormberg Group archives ~50 million years of geological history in <1.3 km of maximum stratal thickness, whereas the Beaufort Group represents ~26 million years of geological history in >4.5 km of thickness in the central MKB (see the Karoo timewheel: Fig. 1c). Regardless of the resolution of the geological archive provided by the Stormberg Group, establishing a modern chronostratigraphic framework for the section that encompasses the TJB in southern Africa is long overdue (Figs. 1, 2; e.g., Porro et al., 2010; Sciscio et al., 2017a; McPhee et al., 2017).

The depositional ages of the Stormberg Group formations (Fig. 2) are constrained to some extent by biostratigraphy and, to a lesser extent, magnetostratigraphy. The oldest Stormberg Group unit, the Molteno Formation, is assumed to be Carnian, an assignment based on its exceptionally well-preserved and diverse plant fossil assemblages that are dominated by the seed fern *Dicroidium* (Figs. 2, 3; Anderson and Anderson, 1970; Anderson et al., 1998; Knoll, 2004; Labandeira et al., 2018). Based on biostratigraphic correlations with better-dated global deposits, the two subdivisions of the unconformably overlying Elliot Formation, the lEF and uEF, are believed to be Norian–Rhaetian and Hettangian–Sinemurian, respectively (for lEF see e.g., Hopson, 1984; Gow and Hancox, 1993; Lucas and Hancox, 2001; Knoll 2004; McPhee et al., 2017; for the uEF see e.g., Olsen and Galton, 1984; Smith and Kitching, 1997; Lucas and Hancox, 2001; Knoll, 2005). The overall Norian–Sinemurian age for the Elliot Formation has been confirmed recently via magnetostratigraphy (Sciscio et al., 2017a). The youngest Stormberg Group unit, the Clarens Formation, contains a paucispecific assemblage composed of taxa similar or identical to those common in the underlying uEF, and is inferred to be Sinemurian–Pliensbachian. The age of the upper boundary of the Stormberg Group succession is provided by the conformably overlying, Toarcian-aged continental flood basalts, the outpouring of which terminated sedimentation of the Karoo Supergroup (Figs. 2, 3). Radioisotopic dating of these basalts indicates that the main pulse of this multi-peak volcanic event occurred between 181–183 Ma (Duncan et al., 1997; Svensen et al., 2012; Sell et al., 2014; Moulin et al., 2017). Moreover, field and radioisotopic evidence indicate that the outpouring of the first lava flows, at least in the southern MKB, started a few million years earlier in the late Pliensbachian (at ~189 Ma; Fig. 2; Moulin et al., 2017).

Here we present the first chronostratigraphic framework for the upper Stormberg Group, using new age constraints (maximum depositional ages, MDAs) obtained from detrital zircons in tuffaceous sandstones and siltstones via U-Pb geochronological methods (CA-ID-TIMS, LA-ICP-MS). We regard this initial, basin-wide chronostratigraphic framework as an important independent test of previous age determination methods, while acknowledging that it is but a first step in solving a temporally and geographically enormous problem. Our efforts to arrive at the most accurate age interpretations of these newly obtained geochronological dates are informed by our collective lithostratigraphic, sedimentologic, magnetostratigraphic, and biostratigraphic (including ichnologic) perspectives. Therefore, we also present a brief review of the unit on the basis of these multidisciplinary aspects and integrate the new dates into the overall stratigraphy of the Elliot and Clarens formations. While our dating results are circumscribed by the long duration and limited rock volume of the upper Stormberg Group, this synthesis allows us to infer that the duration of the Elliot depositional episode was middle Norian–Sinemurian, whereas the Clarens depositional episode was mostly Pliensbachian, and thus to evaluate paleobiogeographical signals at the onset and recovery from the ETME. Moreover, these new geochronological dates provide initial steps towards a more quantitative understanding of the rates of sediment preservation, basin evolution processes (e.g., sediment sources, dispersal patterns), paleogeographic/climatic changes, and major paleobiological events, including the tempo and mode of early dinosaur, crocodylomorph, testudinate and mammalian evolution in southern Pangea during the transition from the Late Triassic to the Early Jurassic.

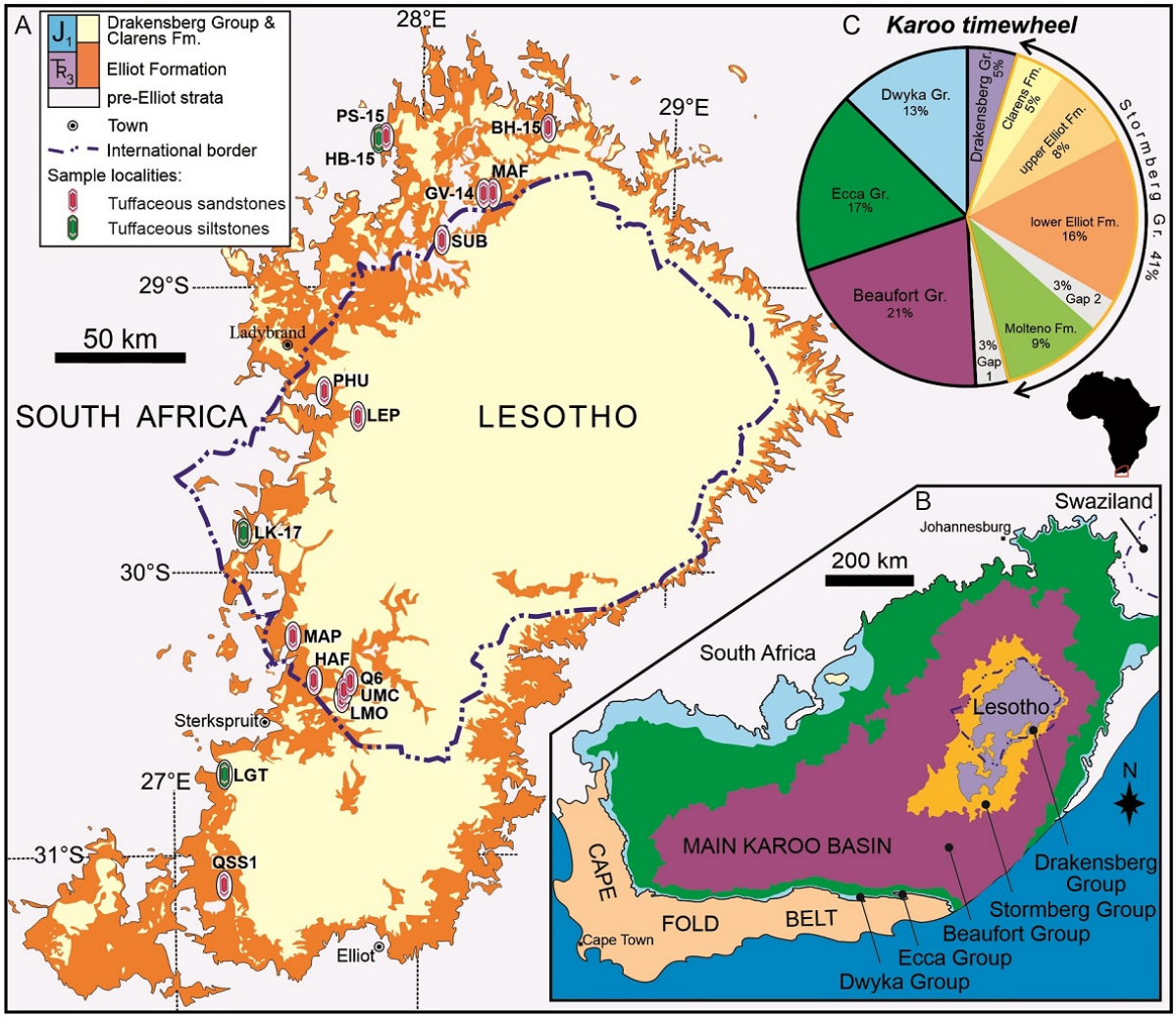

Figure 1. (A) Overview geological map of the upper Karoo Supergroup showing the geographic distribution of the 16 detrital zircon samples presented in this study (see Sections 3 and 4.1 for details). (B) Inset map of the MKB of South Africa and Lesotho showing the position of the Stormberg Group within it. (C) Karoo timewheel showing the relative length of geological time represented by each main stratigraphic unit in the Karoo Supergroup. [final size: full page width, portrait]

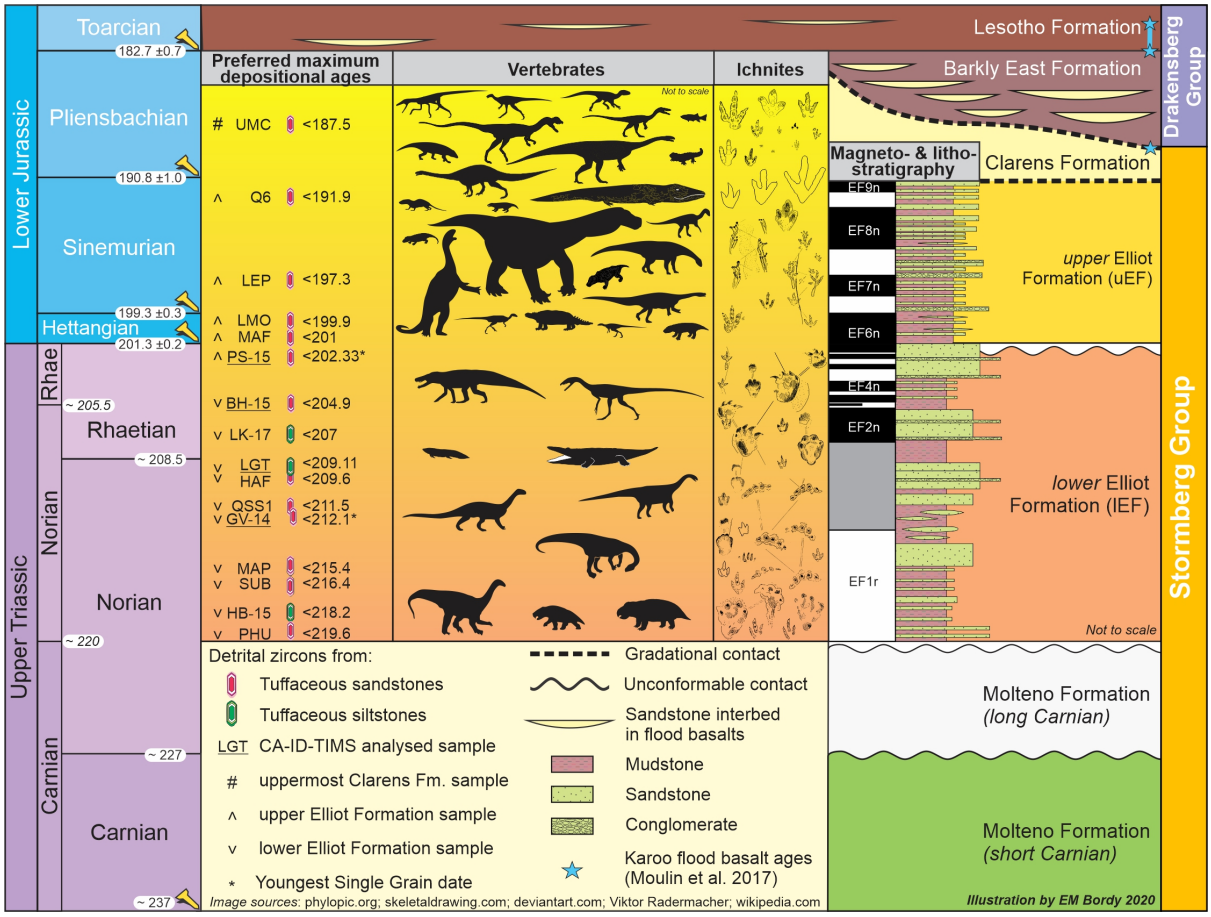

Figure 2. The chronostratigraphy of the Upper Triassic–Lower Jurassic Stormberg and Drakensberg groups (Karoo Supergroup), with special focus on the magneto- and lithostratigraphy of the Elliot Formation, and the main body and trace fossil groups in the upper Stormberg Group. Radioisotopic dates are from this study for the upper Stormberg Group and Moulin et al. (2017; K-Ar, $^{40}Ar/^{39}Ar$ methods) for the Drakensberg basalts. Unless otherwise marked, the maximum depositional ages are based on the mean U-Pb detrital zircon dates of the youngest two or more grains with overlapping dates at 2σ (see Table 1). The less-than sign next to each MDA indicates that the age of the sample could be younger (i.e., the MDAs are only maximum constraints on the age of deposition). Geological time scale based on the International Chronostratigraphic Chart (v2018/08; ICS, 2018) and Cohen et al. (2013). The Triassic time scale shows both the 'long Norian' and 'short Norian' calibrations of the Late Triassic (see discussion in Lucas, 2018). Note that most lithostratigraphic boundaries are likely to be diachronous, i.e., they are time-transgressive laterally across the basin from south to north and likely from west to east as well. Stormberg Group sample locations are shown in Figure 1. For the complete geochronologic dataset, see Supplemental Text 1, Table S1 and Figure S1. For a key to the animal silhouettes and ichnites (mostly from Ellenberger 1970), see Supplemental Text 1. [final size: full page width, landscape]

2. Stratigraphic background

The ETME is one of the 'Big Five' biotic crises that are generally thought to have shaped large-scale patterns of Phanerozoic biodiversity, fundamentally reorganising the taxonomic compositions of both continental and marine biogeographic realms (e.g., Raup and Sepkoski, 1982). Studying the effects of this global event in continental ecosystems is difficult because fossiliferous deposits spanning the Late Triassic–Early Jurassic (specifically the post-Carnian to pre-Toarcian interval) are rare and generally poorly dated (e.g., Lucas, 2018). The Elliot and Clarens formations of southern Africa have rich records of tetrapod body and trace fossils resulting from over a century and a half of investigation (e.g., Owen, 1854; Haughton, 1924; Crompton and Jenkins, 1968; Ellenberger, 1970, 1972, 1974; Kitching and Raath, 1984; Warren and Damiani, 1999; Yates and Kitching, 2003; Knoll, 2004, 2005; Butler et al., 2007; Yates, 2007a, b; Yates et al., 2009; McPhee et al., 2014, 2015a, b; 2017, 2018; Dollman et al., 2017). However, the current state of its chronostratigraphic framework leaves the quantification of geological and biological processes uncertain. The lack of absolute age control in the upper Stormberg Group hampers our ability to accurately and precisely correlate the changes that have already been observed in basin development, ancient landscapes, climate, and faunal assemblages with other global records, as well as with regards to the position of the ETME. In the following sections, we review these and additional limitations of the currently weak chronostratigraphic framework, and highlight the recent advancements in the various stratigraphic studies of the Elliot Formation, the unit that contains the Triassic-Jurassic boundary in southern Africa.

2.1. Lithostratigraphy

The first modern facies analysis study of the Elliot Formation confirmed that the informal lithostratigraphic subdivisions of the unit (lEF and uEF, respectively) are recognizable on a basinal scale (Figs. 2, 3; Bordy et al., 2004a, b, c, 2005). These studies also demonstrated mappable regional spatiotemporal changes in facies distribution, thickness, and sediment dispersal patterns (via provenance assessment of paleocurrents and source rock composition) in this fluvio-lacustrine succession. Although lithostratigraphic/sedimentary facies characteristics (summarized in Figure 3) assist in the straightforward separation of the lEF and uEF, the lateral variability of the stratigraphic architecture at outcrop scale is so high throughout the basin that robust correlation between facies associations is not feasible even in adjacent, high-quality outcrops. Although the correlation of fluvio-lacustrine strata is usually problematic (e.g., Miall, 2013, 2015, 2016), the absence of high-

resolution subsurface data (e.g., seismic reflection studies, core data) for the entire Stormberg Group further compound these correlation difficulties.

The lEF is generally characterised by heterogeneous red-purple (ranging from olive-grey to bluish-to-purplish-red) mudstone units with rare colour mottling, and multi-storey, cliff-forming sandstone units with well-developed lateral accretion surfaces and irregular, erosive basal bounding surfaces (Fig. 3; Bordy et al., 2004b, d). The medium-grained, litho-quartzose sandstones in the lEF can be up to ~20 m thick, and have asymmetrical geometry in cross-section perpendicular to paleocurrent directions. The sandstones are often trough and planar cross-bedded and massive (structureless); low-angle cross-bedding and planar stratification (horizontal lamination) are rare. Ripple cross-lamination, bioturbation structures and soft-sediment deformation features are all extremely rare. Well-defined, upward-fining successions often begin with mud-pebble conglomerate lags. The mudstones, which are 20–30 m thick on average, rarely display pedogenic alteration features (e.g., irregular mottles, desiccation cracks, carbonate nodules) in contrast to uEF mudstones.

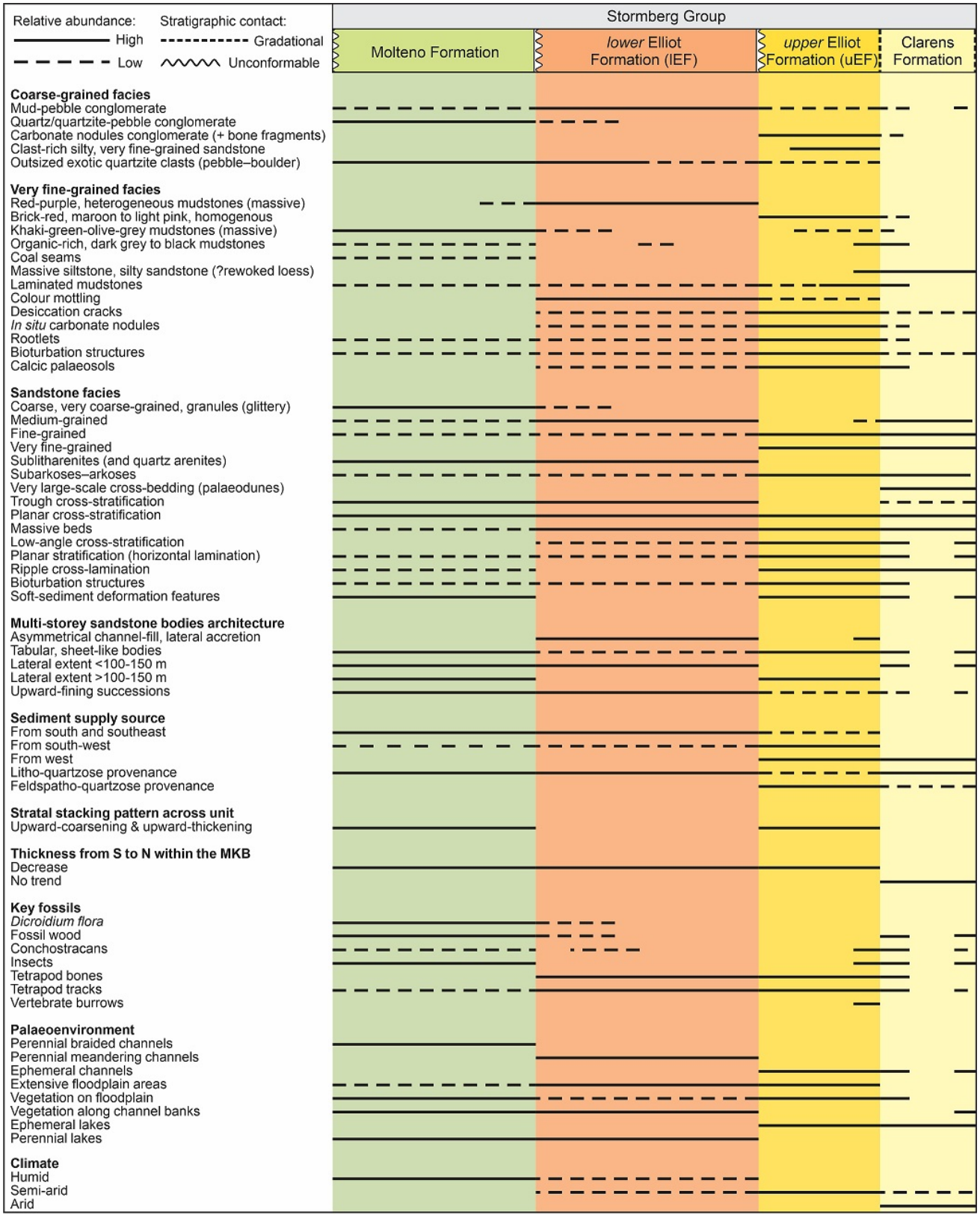

Figure 3. Sedimentary facies characteristics and main depositional conditions of the Molteno, lEF, uEF and Clarens formations (Stormberg Group) in the main Karoo Basin of southern Africa. (Data sources: Ellenberger et al., 1964; Bordy et al., 2004a, b, c, d, 2005; Bordy and Head, 2018). [final size: full page width, portrait]

The majority of the uEF comprises very fine- to fine-grained, feldspatho-quartzose sandstones and pedogenically altered mudstones (mostly siltstones) (Fig. 3; Bordy et al., 2004b; McPhee et al., 2018). The diagnostic sedimentary facies of the uEF are intraformational conglomerates, consisting mostly of reworked pedogenic nodules and bone fragments, and clast-rich, massive, silty, very fine-grained sandstones (e.g., Bordy et al., 2004b: pp. 393, 395, 397; Bordy et al., 2017a: pp. 366, 369). The uEF sandstones are tabular, sheet-like bodies with thickness ranges of < 1–6 m that can extend laterally for several hundred metres (Fig. 3). The uEF sandstones contain planar stratification (horizontal lamination), ripple cross-lamination and, less commonly, planar cross-bedding. Soft sediment deformation and bioturbation structures are common. In the uppermost uEF, sandstones are slightly coarser, medium-grained and occur as channel-shaped bodies with rare lateral accretion beds that are up to 15 m in thickness, resulting in an overall upward-coarsening and upward-thickening character. The uEF mudstones are brick-red, maroon to light pink in colour, and regularly show evidence for pedogenic overprinting (e.g., desiccation cracks, in-situ carbonate nodules, rootlets, colour mottling, bioturbation structures) in contrast to the lEF mudstones. Laminated mudstones, appearing dark grey to black, are also present in the uEF. They are rich in organic matter and some bear conchostracans in the uppermost uEF (e.g., Sciscio et al., 2017b; Rampersadh et al., 2018).

Sediment supply patterns prevailed from the south in the lEF but were replaced by transportation directions mainly from west and south-west in the uEF (Fig. 3). Simultaneously, with the reorganization of the sediment supply patterns, the source of the sandstones also shifted from a litho-quartzose provenance in the lEF to a feldspatho-quartzose one in the uEF. Both the lEF and uEF show a decrease in thickness from south to north within the MKB, especially over the southern margin of the Kaapvaal Craton. This south-to-north thinning is particularly distinct in the lEF, which is ~300 m-thick near its type locality in the Barkly Pass, and <10 m-thick in the northernmost region of the basin (e.g., Bordy et al, 2004b, c; Bordy and Eriksson, 2015; McPhee et al., 2017). The uEF has a maximum thickness of ~255 m in the south and a minimum thickness of <30 m in the north.

The marked differences in the architecture of the sedimentary facies (i.e., contrasting sandstone body geometries and associated facies assemblages), sediment supply pattern, petrological composition and thickness trends at the lEF-uEF contact are explained by changes in fluvial style and regional basin dynamics (Bordy et al., 2004a, b, c, d, 2005). The multi-storey, cliff-forming, asymmetrical channel-fill sandstones of the lEF are interpreted as deposits of a perennial fluvio-lacustrine system that formed under humid to semi-arid climatic conditions. The moderately

meandering channels in the lEF were adorned by riparian forests separated from one another by extensive overbank floodplain areas. In contrast to the lEF, the low-energy depositional system in the uEF was prone to cycles of sudden flash flooding and prolonged desiccation under semi-arid climatic conditions. The multi-storey, mostly tabular sandstones in the uEF formed in ephemeral watercourses, which intermittently flowed on vast floodplains with abundant calcic paleosols and shallow, mostly ephemeral lakes. A long-term trend of aridification that started in the uEF (e.g., Bordy et al, 2004b; Bordy and Erikson, 2015; Sciscio and Bordy, 2016) continued during the deposition of the Clarens Formation (Figs. 2, 3), which is dominated by massive to large-scale, cross-bedded sandstones that formed in wet and dry deserts with large, down-wind and eastward migrating sand dunes (e.g., Beukes, 1970; Visser, 1984; Eriksson, 1986; Bordy and Head, 2018).

The contrast in fluvial style, provenance and thickness trends across the contact of the lEF and uEF was interpreted by Bordy et al. (2004a, b, c, d, 2005) as a basin-wide unconformity. The duration of this stratigraphic gap was sufficiently long to have allowed the reorganization of regional fluvial depositional style and drainage patterns. Neither the absolute time represented by this regionally mappable paraconformity (essentially a sequence boundary) nor its date of occurrence relative to the TJB have been quantified, mainly because the aforementioned lithostratigraphic and sedimentologic methods are unsuitable for age assessments, except for coarse inferences of relative rates of sediment preservation (e.g., mature paleosols develop during prolonged low rates of clastic sediment accumulation vs flash flood sediments representing sudden high rates of accumulation).

2.2. Magnetostratigraphy

Magnetostratigraphy is a stratigraphic correlation and relative dating tool that can provide an autonomous framework for delineating discrepancies between other stratigraphic correlation methods. However, in fluvio-lacustrine units (such as the Elliot Formation), magnetostratigraphy is fraught with uncertainty due to the inherently discontinuous nature and heterogenous stratigraphic architecture of such sedimentary rock successions (e.g., Miall, 2013). To minimize analytical and stratigraphic uncertainties, modern magnetostratigraphic approaches combine detailed litho- and biostratigraphic assessments with robust age constraints, which serve as stratigraphic calibration and anchoring points (e.g., Tauxe, 1998; Langereis et al., 2010).

Paleomagnetic studies in the Mesozoic of southern Africa have relatively low resolution and mostly focus on the Permo-Triassic boundary and Toarcian continental flood basalts (e.g. de Kock and Kirsvinch, 2004; Lanci et al., 2013; Moulin et al., 2011, 2012, 2017). Magnetostratigraphic studies on

the upper Stormberg Group are less common (e.g., Opdyke, 1964; de Kock, 2003; Sciscio, 2016; Sciscio et al., 2017a), and use magneto- and biostratigraphic correlations to link this succession to its global counterparts in continental settings. For example, Sciscio et al. (2017a) built a 280-m-thick composite magnetostratigraphic section for the Elliot Formation by combining nine stratigraphic sections along a ~350-km-long transect in the MKB (Figs. 1, 2). This composite section comprises seven polarity pairs (EF2–EF8) and two single polarity intervals (EF1r and EF9n). The lEF contains four normal-reverse polarity intervals (EF2–EF5) and one reverse polarity zone (EF1r). The uEF has three normal-reverse polarity intervals (EF6–EF8) and one normal polarity zone (EF9n). The basal magnetostratigraphic tie is a single ^{40}Ar-^{39}Ar age of 215±3 Ma (Hälbich et al., 1983), which has been tentatively linked to a deformation event in the Cape Fold Belt (Catuneanu et al., 1998) and to the unconformable contact between the Molteno and Elliot formations (Bordy et al., 2005). This age has been debated by various authors (e.g., Duane and Brown, 1992; Hansma et al., 2015; Blewett and Phillips, 2016; Blewett et al., 2019), and is generally considered to be unreliable. The uppermost tie point is the radioisotopic age and magnetostratigraphy established for the Toarcian continental flood basalts (e.g., Duncan et al., 1997; Moulin et al., 2011, 2012, 2017). Augmented with biostratigraphic proxies, Sciscio et al. (2017a) also attempted a global correlation of the Elliot Formation to continental sections in the North American Newark APTS, Hartford Basin, Chinle and Moenave formations of the Colorado Plateau (e.g., Nevada, Utah, northern Arizona, western New Mexico), the Argentinian Ischigualasto–Villa Union Basin, and the European St Audrie's Bay (UK) and Paris Basin (France) (e.g., Moreau et al., 2002; Donohoo-Hurley et al., 2010; Olsen et al., 2010; Zeigler and Geissman, 2011; Hüsing et al., 2014; Kent et al., 2014).

Sciscio et al. (2017a) emphasized that the magnetozones have an inconsistent thickness between sections given isopach changes across the basin, which are due to the variable sedimentation rates and the erosional events typical in fluvio-lacustrine environments. Although the basin-wide unconformity between the lEF and uEF is of unknown duration, it has been recognized to have impacted the magnetostratigraphic correlations. Moreover, the main caveat of Sciscio et al. (2017a) is the need for reliable radioisotopic calibration points, and a revision of the current biostratigraphic framework of the Elliot Formation. Therefore, the reliability of the composite magnetostratigraphic section is expected to increase with the addition of new multi-disciplinary datasets.

306 **2.3. Biostratigraphy**

307 The Elliot Formation preserves a series of exemplary Late Triassic–Early Jurassic continental faunas
308 (Fig. 2) that have been the subject of several in-depth reviews (e.g., Haughton, 1924; Ellenberger,
309 1970; Kitching and Raath, 1984; Knoll, 2004, 2005; McPhee et al., 2017; Viglietti et al., in press a, b).
310 We summarize these below and present the preliminary findings of a quantitative investigation into
311 the geospatial and stratigraphic distributions of upper Stormberg Group vertebrate taxa in Sections
312 3.2 and 4.2 (see also Viglietti et al., in press a, b).

313 The lEF is similarly fossiliferous, but less taxonomically diverse than the uEF, and is dominated by
314 early branching sauropodomorph dinosaurs (Fig. 2). Following McPhee et al. (2017), this assemblage
315 includes the following valid sauropodomorph genera: *Plateosauravus* (Haughton, 1924; Yates, 2003),
316 *Eucnemesaurus* (Van Hoepen, 1920; Yates, 2007a; McPhee et al., 2015a), and *Blikanasaurus* (Galton
317 and Van Heerden, 1985). *Melanorosaurus* is provisionally retained as a fourth valid sauropodomorph
318 taxon on the basis of its syntype material (Haughton, 1924; Galton et al., 2005; Yates, 2007b; PMB
319 and JNC, unpublished results), although its taxonomic validity and the referral of key specimens have
320 been questioned (McPhee et al., 2015a, b, 2017). It is clearly in need of substantial revision and this
321 work is currently in progress (PMB and JNC, unpublished results). Additionally, although the recently
322 named *Sefapanosaurus* (Otero et al., 2015) and *Meroktenos* (Gauffre, 1993; de Fabrègues and Allain,
323 2016) have poor provenance data, these might also represent valid lEF taxa. As concluded by
324 McPhee et al. (2017), determining clear morphological boundaries between lEF sauropodomorphs is
325 far from straightforward, with all known taxa possessing medium-to-large bodied, variably robust
326 phenotypes that are currently distinguished by subtle postcranial features (cranial remains are
327 currently unknown for all named species). Although tridactyl theropod trackways are well-known in
328 the lEF (see Section 2.4), the only body fossil evidence for theropods thus far comes from isolated
329 teeth (e.g., Ray and Chinsamy, 2002), which are very difficult to distinguish from those of
330 carnivorous pseudosuchians. There are currently no ornithischian dinosaurs in the lEF (see
331 comments on *Eocursor*, below and Section 5.4.3).

332 Therapsids in the lEF are represented by the traversodontid cynodont *Scalenodontoides*
333 *macrodontes* (Crompton and Ellenberger, 1957), the youngest known traversodontid occurrence in
334 Gondwana (Abdala and Gaetano, 2018). Recent work added the tritheledontid cynodont
335 *Elliotherium kersteni* (Sidor and Hancox, 2006) and a possible diademodontid cynodont (Abdala et
336 al., 2007) to this list. However, the diademodontid site has been reassigned to the uEF (Bordy et al.,
337 2017a) and we consider it very likely that the *Elliotherium kersteni* is from a bed in the lower uEF as
338 this taxa is associated with other fossils and rock types that are typical in the uEF (EMB and PAV,

unpublished results). Although the ichnofossil record has hinted at the presence of large dicynodonts in the lEF (see Bordy et al., 2017b for a summary), this was only confirmed recently with the description of *Pentasaurus goggai* (Kammerer, 2018), and the discovery of new, currently unpublished fragmentary dicynodont material from Eastern Cape Province (JNC, PAV, LS, unpublished data).

Pseudosuchian archosaurs have an enigmatic presence within the lEF. Previous reports of aetosaurs (e.g., Kitching and Raath, 1984) have been shown to be spurious (Tolchard et al., 2019). Maxillary and dentary fragments of likely two species of 'rauisuchians' (i.e., non-crocodylomorph pseudosuchians branching later than aetosaurs) were recently identified by Tolchard et al. (2019), but their exact provenance is unknown. It is possible that isolated occurrences of serrated, recurved teeth indicates the presence of carnivorous pseudosuchians, such as poposauroids or non-crocodylomorph loricatans (e.g., '*Basutodon*', Huene, 1932; see also Tolchard et al., 2019) but, as noted above, a possible theropod identity cannot be discounted. Although never adequately studied, some of the material collected as part of the '*Aliwalia rex*' (Galton, 1985) assemblage is possibly non-crocodylomorph pseudosuchian in origin, and could explain why material otherwise referable to Sauropodomorpha might have been incorrectly interpreted as a 'herrerasaurid theropod' (see Yates, 2007a).

The final major tetrapod group within the lEF is temnospondyl amphibians. This fauna was most recently reviewed by Warren and Damiani (1999) who noted the presence of several indeterminate stereospondyls all referable to chigutisaurids, which discounts evidence of capitosaurids from the lEF (Kitching and Raath, 1984). Based on our recent field investigations and consultation with the original collector (B. Battail, personal communication, 2018), we confirm that the stratigraphic position of a gigantic brachyopid stereospondyl mentioned by Steyer and Damiani (2005) originated from the lower uEF near Alwyns Kop in Lesotho.

In contrast to the lEF, the uEF and Clarens Formation sauropodomorph assemblage is morphologically and taxonomically diverse (Fig. 2), and contains the following valid genera: *Massospondylus* (Cooper, 1981; Gow et al., 1990; Yates and Barrett, 2010; Chapelle and Choiniere, 2018; Barrett et al., 2019), *Antetonitrus* (Yates and Kitching, 2003; McPhee et al., 2014), *Aardonyx* (Yates et al., 2010), *Pulanesaura* (McPhee et al., 2015b; McPhee and Choiniere, 2017), *Ngwevu* (Chapelle et al., 2019) and *Ledumahadi* (McPhee et al., 2018). Together these taxa comprise a diverse fauna ranging from gracile massospondylids to multi-tonne lessemsaurids, signalling disparate feeding ecologies supported by distinct biomechanical strategies (McPhee et al., 2015b, 2017, 2018). The discovery of *Pulanesaura* also indicates the presence of the earliest branching

sauropods (McPhee et al., 2015b). Two other genera, *Arcusaurus* (Yates et al., 2011) and *Ignavusaurus* (Knoll, 2010) have also been named from the uEF in recent years, but their validity has been questioned (e.g., Yates et al., 2011; McPhee et al., 2017).

Theropod dinosaurs in the uEF and Clarens Formation are represented by fragmentary remains attributed to the southern African coelophysid *Megapnosaurus rhodesiensis* (formerly *Syntarsus rhodesiensis* and *Coelophysis rhodesiensis*, see below; Kitching and Raath, 1984; Smith and Kitching, 1997; Munyikwa and Raath, 1999; Bristowe and Raath, 2004). A larger theropod species, *Dracovenator regenti,* was named from partial cranial material and is possibly related to the North American taxon *Dilophosaurus* (Yates, 2005). Several genera of basal ornithischian dinosaur have been named from the uEF, including some of the earliest global occurrences of the group. *Lesothosaurus diagnosticus* (e.g., Galton, 1972; Butler, 2005; Porro et al., 2015; Barrett et al., 2016; Baron et al., 2016, 2017a; Sciscio et al., 2017c) represents the most abundant form (*Stormbergia dangershoeki* is currently thought to be a junior synonym of this taxon: e.g., Baron et al., 2017a; Sciscio et al., 2017c). Several heterodontosaurids are also known (Porro et al., 2010), including: *Heterodontosaurus tucki* (e.g., Crompton and Charig, 1962; Norman et al., 2011; Sereno, 2012), *Abrictosaurus consors* (Thulborn, 1974; Sereno, 2012), *Lycorhinus angustidens* and *Pegomastax africanus* (Butler et al., 2008; Sereno, 2012). *Eocursor parvus*, originally described as a lEF taxon (Butler et al., 2007), has recently been reinterpreted as coming from the uEF (Olsen et al., 2010; McPhee et al., 2017).

The most abundant uEF taxa after dinosaurs are cynodonts, of which both non-mammaliaforms and mammaliaforms are present. Following the recent review of Abdala and Gaetano (2018), the former includes the tritheledontid taxa *Tritheledon, Diarthrognathus* and *Pachygenelus,* and the tritylodontids *Tritylodontoideus* and *Tritylodon*. Mammaliaformes are represented by the morganucodontids *Megazostrodon* and *Erythrotherium.*

The diverse uEF crocodylomorph fauna was recently reviewed by Dollman et al. (2017), with the following taxa recognised currently: the non-crocodyliform crocodylomorphs *Sphenosuchus acutus* and *Litargosuchus leptorhynchus*; and the crocodyliform 'protosuchids' *Protosuchus haughtoni*, *Notochampsa istedana* and *Orthosuchus stormbergi*. Dollman et al. (2017) noted that the majority of crocodylomorph occurrences are restricted to the upper half of the uEF. Non-archosaurian reptiles are represented by the early turtle *Australochelys africanus* (Gaffney and Kitching, 1994) and a specimen of the rhynchocephalian *Clevosaurus* sp. (Sues and Reisz, 1995). As with the lEF, the temnospondyl record of the uEF is restricted to mostly indeterminate remains of chigutisaurid

stereospondyls (Warren and Damiani, 1999), one of which is the largest brachyopid stereospondyl documented to-date (Steyer and Damiani, 2005), as noted above.

2.3.1 Biostratigraphic correlations

Global biostratigraphic correlations for Stormberg Group vertebrate faunas are based on weak evidence. Many rely on broad faunal similarities, or 'stage of evolution' arguments, rather than the presence of shared index taxa, leading to low precision, issues of replicability between different workers, and decreased confidence in their results (e.g., Olsen and Sues, 1986; Lucas, 1998; see Rayfield at al., 2009 for a critique of this approach). No species-level taxa in the Stormberg Group are shared with non-African faunas, only four genera are shared, and phylogenies including Stormberg taxa at the species level are either labile, weakly supported, or have not been performed.

The poorly known lEF fauna has been biostratigraphically correlated, often tentatively, with Norian–Rhaetian faunas such those from the 'Middle Keuper' of Germany, the Los Colorados Formation of Argentina, and the Chinle Formation of the USA (Lucas and Hancox, 2001; Knoll, 2004; McPhee et al., 2017). However, the absence of shared index taxa does not allow for a precise correlation with these deposits. The fauna of the uEF and Clarens Formation has been correlated with Early Jurassic faunas, such as the Lower Lufeng Formation of China, the Glen Canyon Group of the USA, and the McCoy Brook Formation of Canada (Olsen and Galton, 1984; Smith and Kitching, 1997; Lucas and Hancox, 2001; Knoll, 2005) and, in this case, some potentially useful shared taxa are present. For example, the close similarity of species within the crocodyliform genus *Protosuchus* from the uEF (*P. haughtoni*), the Moenave Formation of the Glen Canyon Group, Arizona (*P. richardsoni*: Clark, 1986), and the McCoy Brook Formation, Nova Scotia (*P. micmac*: Sues et al., 1996) does suggest that these deposits are approximately contemporaneous. These North American strata are currently regarded as Hettangian in age on the basis of a radioisotopic date recovered from basalts underlying the McCoy Brook Formation (Sues and Olsen, 2015) and detrital zircon dating of the Moenave Formation (Suarez et al., 2017). Correlation with the McCoy Brook Formation is further supported by the shared genera *Pachygenelus* (a trithelodontid cynodont: Shubin et al., 1991) and *Clevosaurus* (a rhynchocephalian lepidosauromorph: Sues and Reisz, 1995), both of which are absent from the depauperate fauna of the Moenave Formation. The absence of these same genera from the diverse fauna of the Kayenta Formation, which overlies the Moenave Formation, suggests that the fauna of the uEF is older than that of the Kayenta Formation, which has been dated with detrital zircons as no older than late Pliensbachian (Marsh and Rowe, 2018). *Protosuchus* has been reported from the Hettangian of Poland (Gierlinksi and Potemska, 1985), providing a potential European correlation, but the latter requires confirmation given the similarities of this material to other 'protosuchian'

genera. More promisingly, *Clevosaurus* has been recorded from several other Early Jurassic faunas, including the Hettangian of the UK (Evans and Kermack, 1994) and the Early Jurassic of China (Luo and Wu, 1994), extending its potential use in global correlations. However, the stratigraphic range of *Clevosaurus* also extends into the Late Triassic, based on abundant material from the UK, Belgium, Luxembourg and Brazil (Fraser, 1988; Godefroit and Sigogneau-Russell, 1995; Hsiou et al., 2015, 2019). Although these Late Triassic occurrences might offer some support for the proposed Rhaetian age inferred for the lower uEF on the basis of magnetostratigraphy (Sciscio et al., 2017a), it is more likely that they represent species that are temporally distinct (Hsiou et al., 2019), although the monophyly of *Clevosaurus* has recently been questioned (Herrera-Flores et al., 2018; Hsiou et al., 2019). Finally, coelophysoid theropods have been identified in both the Late Triassic (Norian) Chinle Formation of the USA (*Coelophysis bauri*; Colbert, 1989) and the uEF (*Megapnosaurus rhodesiensis*; Munyikwa and Raath, 1999; as '*Syntarsus*' *rhodesiensis* and as '*Coelophysis*' *rhodesiensis* in previous works), although with distinct species in each region. However, anatomically similar coelophysoids are also known from other Lower Jurassic deposits such as the Lufeng Formation of China (You et al., 2014) and the Kayenta Formation of North America (e.g., Rowe, 1989). The inclusion of *M. rhodesiensis* within *Coelophysis* was proposed by Bristowe and Raath (2004), and could potentially indicate correlation with the Chinle Formation. However, recent phylogenetic studies question that assignment (e.g., Ezcurra and Brusatte, 2011; Griffin and Nesbitt, 2019; Wang et al., 2017), and we regard the occurrence of coelophysoids in the uEF as consistent with an either Late Triassic or Early Jurassic age (also see Martínez and Apaldetti, 2017).

Biostratigraphic correlations between other Karoo-aged basins in southern and eastern Africa are also weakly supported due to the absence of shared genus- and species-level taxa. Currently, no lEF vertebrate taxa are known outside the main Karoo Basin. However, *Megapnosaurus rhodesiensis* has been identified in the uEF and the Forest Formation of Zimbabwe (e.g., Raath, 1969; Munyikwa and Raath, 1999), along with more taxonomically tentative records of *Clevosaurus* (Gow, 1977) and *Notochampsa* (Raath, 1981). Moreover, occurrences of the basal sauropodomorph dinosaur *Massospondylus* have been reported in several Zimbabwean basins (e.g., the Mid-Zambezi, Mana Pools, and Tuli basins: Attridge, 1963; Raath et al., 1970; Bond, 1973; Cooper, 1981; Munyikwa, 1997; Rogers et al., 2004) and might provide a direct faunal link, but the material reported from the Zimbabwean localities requires taxonomic reassessment to confirm these proposals (Barrett et al., 2019). A tentative link between the uEF and Karoo-aged strata in the Luangwa Basin of Zambia has been posited on the basis of taxonomically indeterminate sauropodomorph material (Choiniere and Barrett, 2015), but requires additional support.

2.4. Vertebrate ichnology

The Stormberg Group, and in particular its upper part (Fig. 2), contains a diverse and globally important trackway record, with an abundant assemblage of ichnites attributable to herbivorous and carnivorous dinosaurs, dicynodonts, cynodonts, amphibians, crocodylomorphs, and mammaliaforms (e.g., Ellenberger et al., 1964; Ellenberger 1970, 1972, 1974; Raath et al., 1990; Smith et al., 2009; Wilson et al., 2009; Marsicano et al., 2014; Sciscio et al., 2016, 2017c; Abrahams et al., 2017; Bordy et al., 2017b; Rampersadh et al., 2018).

Paul Ellenberger conducted the pioneering work on this record, erecting a great diversity of tetrapod ichnogenera and ichnospecies in addition to establishing an ichnostratigraphic subdivision for the southern Africa Upper Triassic to Lower Jurassic (e.g., Ellenberger, 1970, 1972, 1974). This work introduced the first biozonation scheme for the Stormberg Group (e.g., lEF includes zones A1 – A6; uEF and the Clarens Formation zones A7, B1– B7) and underscored the division of the regional ichnofaunas into two broad biozones that reflect a faunal change equivalent to the turnover in skeletal remains both locally and globally during the Late Triassic to Early Jurassic. Ellenberger's seminal work was revised some 35 years ago by Olsen and Galton (1984), who significantly reduced the number of ichnotaxa through synonymization. While this ichnotaxonomic revision was valuable for pointing out several *nomina dubia*, it also lumped some valid ichnotaxa, which had the unfortunate corollary of decreasing confidence in the value of the southern African ichnofossils for global correlation and regional biodiversity assessments. The shortcomings of this alternative ichnologic framework have to some extent been rectified subsequently by, for example, Lockley et al. (1996, 2004, 2006), Rainforth (2003), Lockley and Gierlinski (2006), D'Orazi Porchetti and Nicosia (2007), and D'Orazi Porchetti et al. (2015, 2017, 2018). Based on these revisions, the currently accepted tetrapod ichnofaunal list for the Upper Triassic lEF includes *Tetrasauropus, ?Lavinipes jaquesi,* and *Pseudotetrasauropus* (quadrupedal and bipedal sauropodomorph dinosaurs), *Grallator* (theropod dinosaur), *Pentasauropus* (dicynodont), *Sauropodopus* (probable rauisuchians, with similarities to *Chirotherium*), *Paratetrasauropus* (crocodylomorph) and cf. *Brachychirotherium* (archosauromorph), whereas for the Lower Jurassic uEF and Clarens Formation contains *Episcopopus* (amphibian), *Batrachopus* (crocodylomorph), *Moyenisauropus* and *Trisauropodiscus* (ornithischians), *Ameghinichnus* (tritylodontid cynodonts), a great variety of ichnotaxa on the *Grallator-Eubrontes* plexus and *Kayentapus* (theropods) as well as tentative *Brasilichnium*-like (mammaliaforms, ?synapsids) tracks. This list is far from complete, and our ongoing ichnologic work is aimed at

updating and refining the Stormberg Group ichnostratigraphic scheme to better reflect the true ichnofaunal diversity and the degree of trackmaker endemism within the Stormberg Group (EMB, unpublished results; Sciscio et al., 2016, 2017c; Abrahams et al., 2017; Bordy et al., 2017b, 2020; Rampersadh et al., 2018).

The vertebrate track record of the Stormberg Group, based on shared ichnofauna elements, has been linked to Late Triassic to Early Jurassic tracks on all continents except Antarctica (for relevant reviews see Olsen and Galton, 1984; D'Orazi Porchetti and Nicosia, 2007; Lucas, 2007; Klein and Lucas, 2010; D'Orazi Porchetti et al., 2015; Citton et al., 2018; Hunt et al., 2018 and references therein). However, the coarse temporal and stratigraphic resolution of the tetrapod footprint record in the upper Stormberg Group, in addition to an outdated regional ichnotaxonomy, limits its utility for fine-scale regional or global correlations, despite the great abundance of ichnites within the succession. As mentioned above, this shortcoming is being addressed systematically by our ongoing research program, and a major review of the upper Stormberg track assemblages, augmented by refined stratigraphic data on existing ichnofossil sites and additional collecting, will be forthcoming. Because the current ichnozonation is in flux, this topic is not discussed further herein.

3. Methodology

3.1 Detrital zircon U-Pb geochronology

Given the dearth of prior radioisotopic constraints for the Stormberg Group, due to the lack of obvious primary volcanic lithologies amenable to radioisotopic dating, we have taken the approach of seeking juvenile zircons from volcanoclastic lithologies. Juvenile zircons, those that show morphological evidence for limited reworking within a sedimentary system, and return ages that are 'close' to the true depositional age (TDA), have been used in similar continental sedimentary rock (e.g., Ramezani et al., 2011) to provide useful maximum age constraints on the timing of sediment accumulation, aiding the revision of the chronostratigraphic frameworks. Detrital zircons were successfully extracted and dated from 16 rock samples taken from the Elliot and Clarens formations in South Africa and Lesotho (Supplemental Table S1). Because primary volcanic tuff layers (i.e., pyroclastics) were not identified in the studied succession, the sampled rocks are exclusively tuffaceous sandstones and siltstones.

Zircons were separated using a modified standard method described by Tucker et al. (2013), which includes rock crushing, panning, and magnetic and heavy liquid separation of minerals. Zircons from

each sample were inspected under optical microscopy and showed mixed morphology ranging from rounded, indicating reworking in a sedimentary environment, to acicular and faceted, with medial melt inclusions, typical of volcanic zircon that has not undergone significant reworking. Zircons were then mounted in resin for laser ablation inductively coupled plasma ionization mass spectrometry (LA-ICP-MS) U-Pb dating, with a subset of samples undergoing LA-ICP-MS mounted on tape. The grains from the youngest population were removed for subsequent high-precision chemical abrasion thermal ionization mass spectrometry (CA-ID-TIMS) U-Pb dating (Supplemental Text 1 and Table S1). Both of these geochronological methods have their advantages, as the LA-ICP-MS method allows for a large number of grains to be analysed, increasing the probability of finding the youngest grains, and the CA-ID-TIMS allows for high-precision analyses and treatment for open-system behavior. We have therefore attempted to take advantage of both these methods. Laser ablation spots were selected after the careful consideration of inclusions, textural features, and cracks within the imaged zircon grains. The geochronological dating procedures are further detailed in Supplemental Text 1.

3.2. Biostratigraphic methods

We collated, to the best of our ability, all metadata relating to fossil collections of upper Stormberg tetrapods including both South African (e.g., Iziko Museum, Evolutionary Studies Institute, Albany Museum, National Museum) and international repositories (e.g., London Natural History Museum, Muséum National d'Histoire Naturelle Paris, Naturhistorisches Museum Wien Vienna) using a combination of publications, online databases, and collections records and archives of field notes obtained directly from museum collections. We cleaned these data (e.g., removing spelling errors in taxon names) using automated means where possible. Geospatial positions and stratigraphic provenance of specimen occurrences were validated by cross-referencing Google Earth, GIS software, field notes, personal measurements of stratigraphic sections at historic fossiliferous sites, and the collection of new, well-georeferenced fossil material. Collation of this large historic dataset resulted in over 1400 records, about 20% of which are georeferenced with high credibility, and located across the northern, eastern, southern, and western extent of the Elliot and Clarens formations in the MKB (see Data Availability section).

4. Results

4.1. Appraisal of the detrital zircon U-Pb geochronology methods

To constrain the maximum depositional age (MDA) of the samples from the Elliot and Clarens formations (Table 1), we explore a range of different age calculations for the data obtained from the analysed detrital zircons in order to assess the sensitivity of the age constraints to our chosen interpretive framework. The complete dataset of geochronological measurements is provided in Supplemental Table S1. The relevant measurements for each sample are illustrated in Figures 2, 4, and 5, and in Supplemental Figure S1. The latter provides, for each sample, the relative-age-probability plots (or probability density plots; PDPs) for zircons < 500 Ma, concordance diagrams for zircons younger than ~250 Ma and plots of the weighted mean dates (at 95% confidence) for zircons younger than ~250 Ma. The sample-by-sample appraisal of the detrital zircon U-Pb geochronology dates and the justification of the preferred MDAs and true depositional ages (TDAs) are in Supplemental Text 1.

Table 1. Summary of the results from the different age estimating methods used in constraining the maximum depositional age (MDA) of the samples from the Elliot and Clarens formations in the upper Stormberg Group. For spatiotemporal distribution of the samples, see Figures 1, 2, 4, and 5. Abbreviations: lEF – lower Elliot Formation; uEF – upper Elliot Formation; tsa – tuffaceous sandstone; tsi – tuffaceous siltstone; um – uppermost; σ – internal error. Ages and errors are in millions of years (Ma). Strike-through indicates that the MDA is too young based on stratigraphic constraints. For justification of the preferred MDAs, see Supplemental Text 1.

			Preferred MDA		YSG		YC1σ(2+)		YC2σ(2+)		YC2σ(3+)		YPP
Sample ID	Method	Lithology & formation	Age	2σ	Age	2σ	Age	2σ	Age	2σ	Age	2σ	Age
BH-15	ID-TIMS	tsa lEF	204,9	0,88	204,02	0,59	205	1,2	204,9	0,17			205
GV-14	ID-TIMS	tsa lEF	212.1	0,19	212.1	0,19							
HAF	LA-ICP-MS	tsa lEF	209,6	1,4	208,2	2,9	209	1,6	209,6	1,4	209,6	1,4	209
HB-15	LA-ICP-MS	tsi lEF	218,2	2	216,5	4,7	518	9,9	218,2	2	518	9,7	520
LEP	LA-ICP-MS	tsa uEF	197,3	2,3	195,7	3,1	239,6	2,7	197,3	2,3	243	1,5	196
LGT	ID-TIMS	tsi lEF	209,11	0,20	~~196,89~~	~~0,94~~	209,11	0,2	208,01	0,86	208,01	0,86	209
LK-17	LA-ICP-MS	tsi lEF	207	5	~~195,7~~	~~5,8~~	207,6	5,1	207	5,1	467	8	207
LMO	LA-ICP-MS	tsa uEF	199,9	2,3	193,9	2,9	199,8	2,1	199,9	2,3	232	2	194
MAF	LA-ICP-MS	tsa uEF	201	2,3	199	3	254	2,8	201	2,3	256,4	1,4	256
MAP	LA-ICP-MS	tsa lEF	215,4	1,9	~~201,1~~	~~2,4~~	~~201~~	~~3,2~~	~~201,2~~	~~1,6~~	215,4	1,1	~~201~~
PHU	LA-ICP-MS	tsa lEF	219,6	2,5	217,6	3,4	242,6	2,2	219,6	2,5	243,1	2	243
PS-15	ID-TIMS	tsa uEF	202,33	0,19	202,33	0,19	217,14	0,14	217,21	0,11	217,21	0,11	217
Q6	LA-ICP-MS	tsa um uEF	191,1	1,5	190	2,4	193,4	1,2	191,9	1,5	467,4	2,5	193
QSS1	LA-ICP-MS	tsa lEF	211,5	2,8	207,5	9	211,5	2,9	211,5	2,9	211,5	2,9	213
SUB	LA-ICP-MS	tsa lEF	216,4	2,4	215,4	3,4	216,4	2,4	216,4	2,4	252	2	216
UMC	LA-ICP-MS	tsa Clarens	187,5	1,6	185,9	2,2	186,7	1,2	187,5	1	187,5	1	187

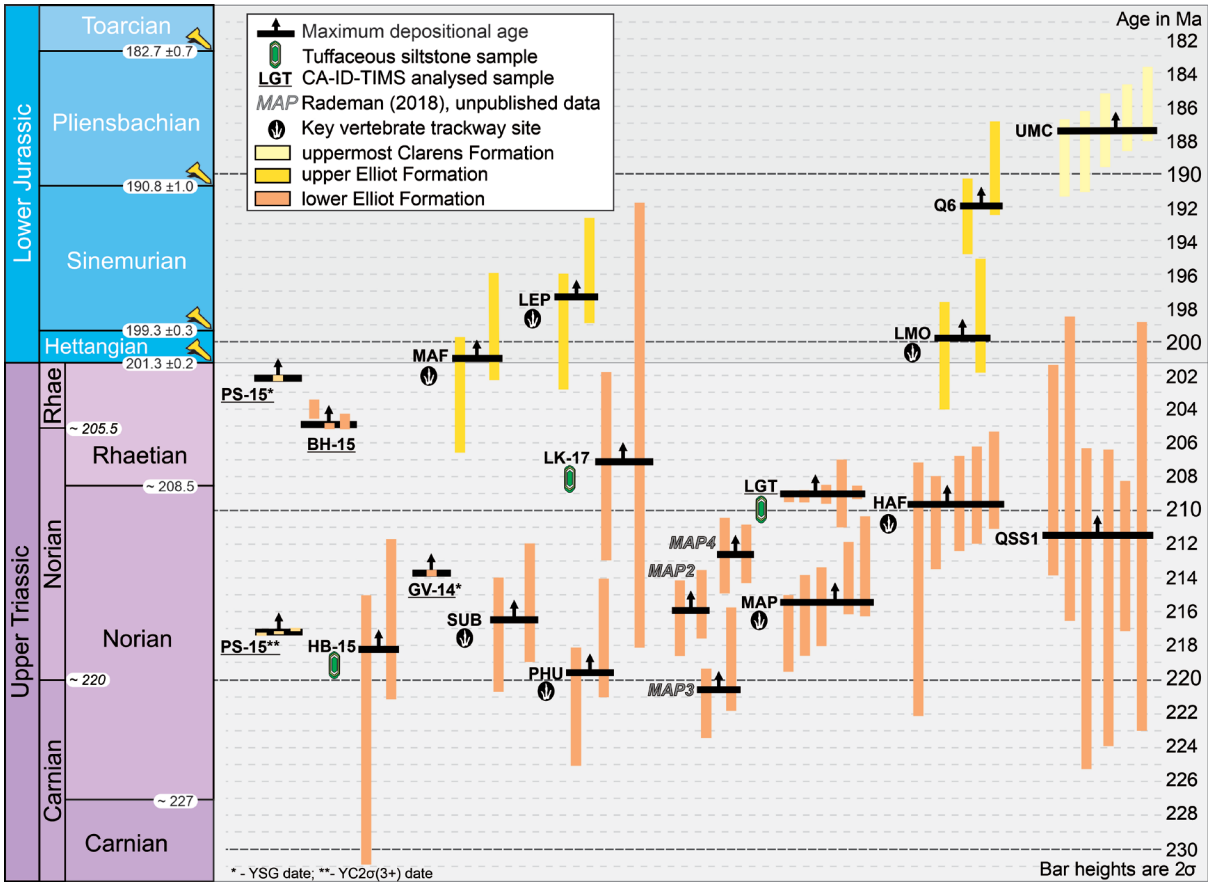

Figure 4. Distribution of the calculated weighted mean dates of the youngest detrital zircon populations (at 95% confidence level) in the analysed samples from the Elliot (15) and Clarens formations (1). Unless otherwise stated on the figure, all ages shown are our preferred MDAs (see Table 1). The arrow pointing forward in time on each MDA line indicates that the age of the sample could be younger (i.e., the MDAs are only maximum constraints on the age of deposition). Bar heights depict 2σ internal analytical uncertainty for each sample. Only detrital zircon dates used in the MDA calculation are depicted; older zircon grain dates are not shown, however, each sample is further illustrated in Supplemental Figure S1. For the complete analytical dataset, see Supplemental Text 1, Table S1 and Figure S1. Sample locations are shown in Figure 1 and corresponding stratigraphic logs are in Figure 5. [final size: full page width, ?portrait]

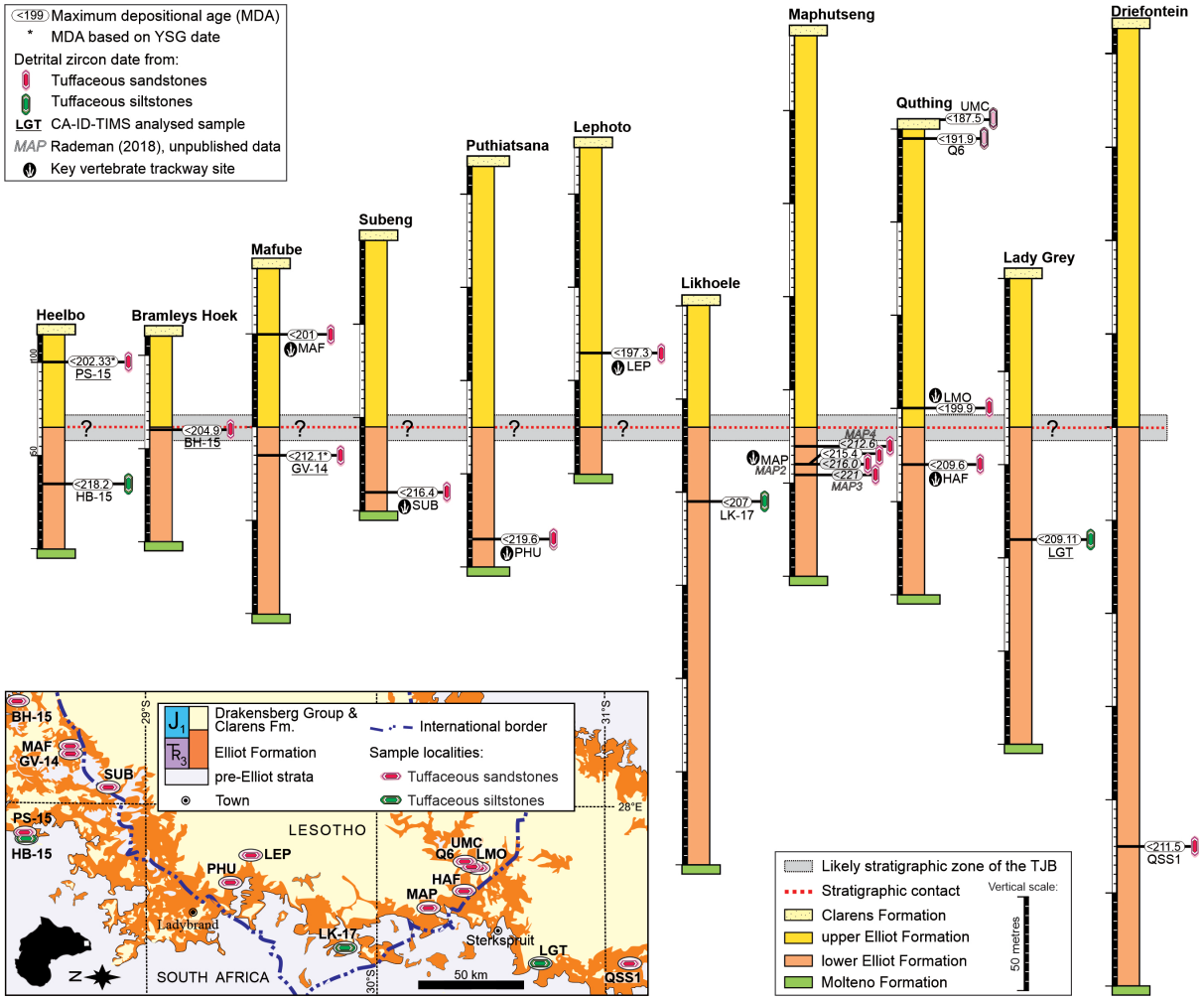

Figure 5. Simplified stratigraphic sections showing the detrital zircon sample position within the local succession. Sections are arranged from north to south (see inset map for locations). Question marks at the stratigraphic contact of the lEF-uEF indicate a <10 m thick zone where lack of outcrops obscure the position of the contact. The uncertain position of the TJB is emphasised by the grey band. The less-than sign next to each MDA indicates that the age of the sample could be younger (i.e., the MDAs are only maximum constraints on the age of deposition). For the complete analytical dataset, see Supplemental Text 1, Table S1 and Figure S1. [final size: full page width, landscape]

Our preferred method for estimating the MDA (Table 1) is the weighted mean of the youngest cluster comprised of two or more grains overlapping with the youngest one at 2σ internal error (YC2σ[2+]). Using two or more analyses instead of the single youngest analysis reduces the chance that the MDA will be younger than the TDA (e.g., as a consequence of Pb-loss; see below). Furthermore, our use of CA-ID-TIMS analyses for a subset of the samples helps deal with this issue – the use of chemical abrasion pre-treatment means that Pb-loss is effectively eliminated, and the higher-precision of the data allow for a more robust assessment of Pb-loss via discordance. Although

somewhat subjective, the use of the YC2σ(2+) metric resulted in the MDA calculations being more consistently compatible with other stratigraphic considerations in the study area. The considerations that are used to constrain our age interpretations include: the stratigraphic context of the sample (i.e., its position relative to key stratigraphic contacts and other dated samples in the same section to which a sample must obey the law of superposition); the location of the sample within the Karoo foreland basin; lithostratigraphic characters of the host rocks (i.e., lEF, uEF); and the body and ichnofossil content of the adjacent strata. In several samples, the youngest single grain method (YSG) seems to be the least representative of the TDA, because the measured dates of the youngest grain often seem younger than the expected TDA than what would be anticipated from other stratigraphic considerations (e.g., samples BH-15, LGT). This is likely due to Pb-loss as explained further in the Supplementary Text 1 (as well as in e.g., Dickinson and Gehrels, 2009; Corfu, 2013; Andersen et al., 2019; Gehrels et al., 2019; Herriott et al., 2019; Rossingnol et al., 2019). To put it differently, the YSG method is statistically the least robust, because it focuses on a single data point that is often not reproducible in detrital zircon samples. The MDA calculations based on age clusters are more robust than the YSG because they incorporate multiple data points and account for internal analytical error and the external error of the population (e.g., Dickenson and Gehrels, 2009; Gehrels et al., 2019; Herriott et al., 2019). Although YC2σ(3+) is the second most quoted MDA metric in the literature (e.g., Coutts et al., 2019), our preferred method for interpreting MDA is its modified version, the YC2σ(2+) metric as explained above. Contrary to the YSG metric, the weighted mean calculated from the youngest grain cluster composed of three or more grains that overlap at 2σ uncertainty (YC2σ[3+]) often appears to be too conservative, yielding older dates (early Middle Triassic – Ordovician) than the currently accepted age estimates of Late Triassic – Early Jurassic for the upper Stormberg Group (e.g., samples HB-15, LK-17). In these cases, it is likely that the measured dates are significantly older than the TDA, because near-depositional-age zircons were not captured in the sediment during deposition or are too few in the sample for this date-calculation method (e.g., Andersen et al., 2016). For more comprehensive discussions on the various MDA calculations used, including their relative merits, the readers are referred to Dickinson and Gehrels (2009), Andersen et al. (2019), Coutts et al. (2019), Gehrels et al. (2019), Herriott et al. (2019), Johnstone et al. (2019), and Rossignol et al. (2019).

4.2. Biostratigraphic results

Several clear patterns emerge from our database of upper Stormberg tetrapod occurrences (Fig. 6). There is a pronounced turnover across the lEF/uEF contact. No currently valid tetrapod genera cross

this boundary, and although it is possible that the dipnoan *Ceratodus* is present in the lEF ('EMB, unpublished material') and uEF (Kitching and Raath, 1984), this genus is temporally wide-ranging and the upper Stormberg material is in need of revision. Family level or higher boundary crossers include Sauropodomorpha, Cynodontia, and Chigutisauridae.

Lower Elliot Formation tetrapod occurrences, in general, are as geographically widespread as those in the uEF (Fig.7), but the lEF has many fewer well-georeferenced records for valid taxa. For example, in the lEF, only *Scalenodontoides*, *Eucnemesaurus*, and possibly *Melanorosaurus* have representative occurrences approximating the geographic range of the overall fossil sample, whereas the uEF has at least five such taxa (*Heterodontosaurus*, *Lesothosaurus*, *Massospondylus*, *Protosuchus, Tritylodon*). In addition, poor taxonomic data for many lEF tetrapod occurrences lead to insufficient ability to infer stratigraphic ranges for most lEF taxa, with the notable exception of *Scalenodontoides* (Viglietti et al., in press a). This traversodontid cynodont is the only lEF tetrapod taxon that is currently taxonomically valid, easy to identify in the field, and known from multiple specimens with well-constrained provenance from several lEF localities across the basin (unlike any of the lEF dinosaur taxa - see e.g., McPhee et al., 2018). In contrast, the uEF is rich in well-georeferenced fossil taxa, providing detailed information for the stratigraphic ranges of most uEF fossil vertebrate lineages (Fig. 7). We also observe a similar trend to that noted by Kitching and Raath (1984), where a sudden increase in the relative abundance of fossils occurs above the lower quarter of the uEF and at the contact of the uEF and Clarens Formation.

Dinosaur lineage diversity increases markedly in the uEF (Fig. 6). Sauropodomorpha are present and relatively abundant in both the lEF and uEF (Fig. 8), although more species are currently known from the uEF. In contrast, ornithischians and non-dental theropod remains are absent from the lEF, indicating that they were either rare or absent. Both groups have their first definite occurrences low in the uEF. Many other tetrapod lineages also make their first appearance in the uEF, with the first crocodylomorphs, probainagnathians (including trithelodontids and tritylodontids), and testudinates appearing relatively low in the uEF and the first mammaliaforms definitively appearing closer to the contact of the uEF and Clarens Formation (Fig. 6).

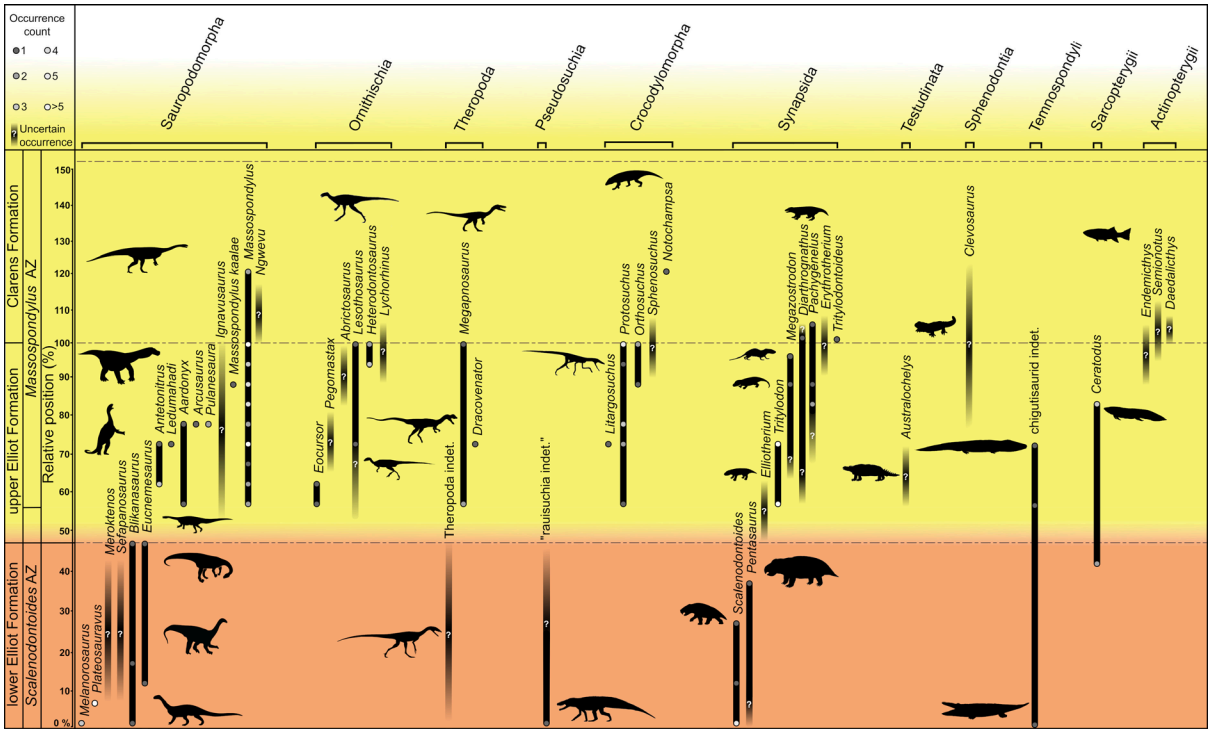

671

672 **Figure 6.** Revised vertebrate biostratigraphy of the Elliot and Clarens formations (upper Stormberg
673 Group) in the MKB. Stratigraphic positions of tetrapod taxa are shown using relative position
674 notation (%) to account for the variable thicknesses of the lower and upper Elliot and Clarens
675 formations. Where poor provenance data is available, the stratigraphic distribution is shaded and
676 identified with a question mark. [final size: full page width, landscape]

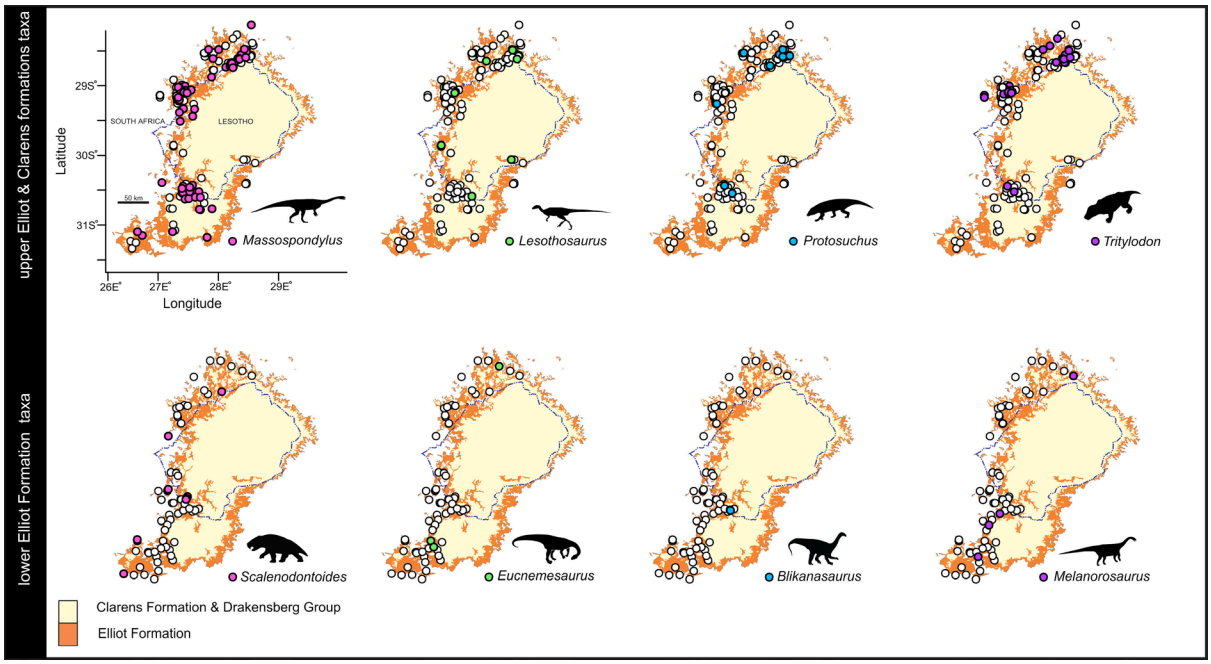

677

Figure 7. Distribution maps of the dominant vertebrate genera in the lEF (lower four panels), and uEF and Clarens formations (upper four panels) in the MKB. Grey circles show the distribution of all known fossil taxa for each unit. Grid system and scale shown for *Massospondylus* applies to all maps. [final size: full page width, landscape]

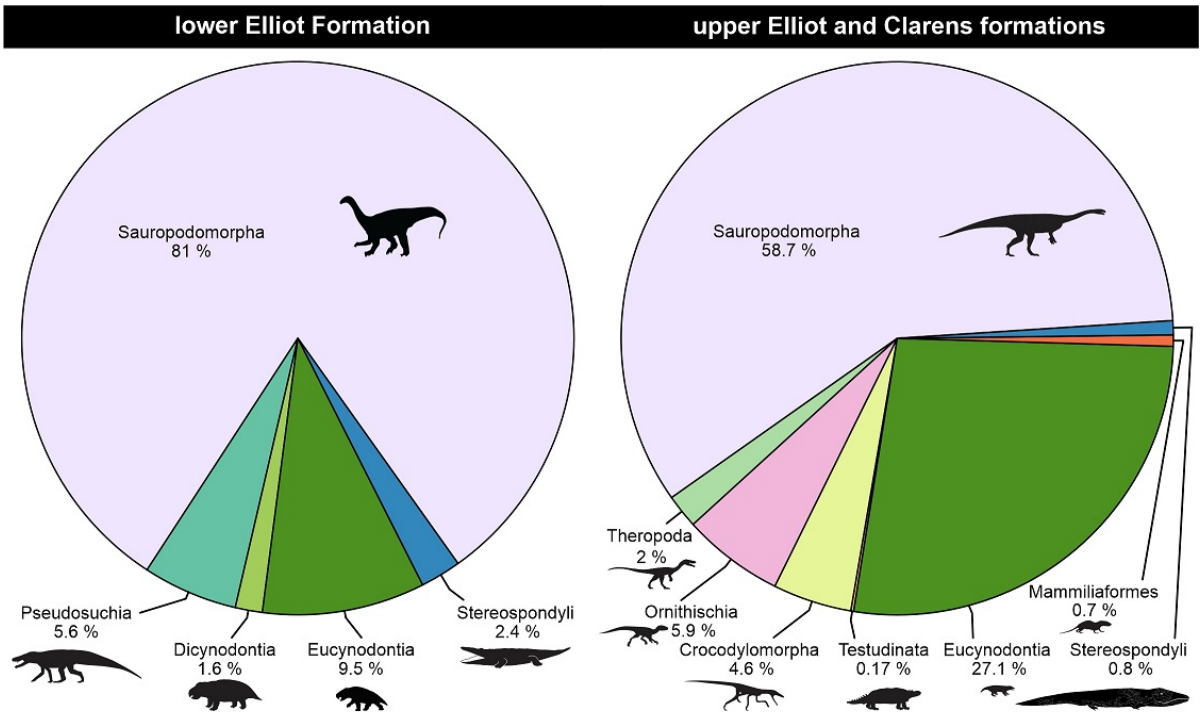

Figure 8. Proportional representation of the key vertebrate taxa in the lEF (left), and uEF and Clarens formations (right) in the MKB. These relative abundances only show occurrences that are identified at genus level. [final size: full page width, portrait]

5. Discussion

5.1. Detrital zircon U-Pb geochronology

In continental rock successions that are lacking pyroclastics (i.e., primary volcaniclastic rocks), utilizing the U-Pb radioisotopic dates from detrital zircons is an effective approach for inferring the maximum depositional ages (MDAs) of strata (e.g., Dickinson and Gehrels, 2009; Ramezani et al., 2011; Coutts et al., 2019; Rossignol et al., 2019). It should be emphasized that the ages of the youngest detrital zircons in any given sedimentary rock sample only provides a maximum constraint on the depositional age; the sample will be younger than the MDA if the detrital zircons are recycled from older sediment sources. The extent to which the youngest detrital zircons provide precise

696 estimates of the true depositional age (TDA) depends on the availability of syn-depositional zircons
697 in the depositional system, typically supplied via windblown volcanic ash or from erosion of active
698 volcanic sources. In some cases, MDA calculations can be older than the TDA even in volcaniclastic
699 sediment due to the presence of antecrystic, epicrystic, and xenocrystic zircon that formed prior to
700 the most recent eruption (Rossignol et al., 2019).

701 Our detrital zircons were recovered from sandstones and tuffaceous siltstones, and both lithologies
702 show evidence of reworking. In this context, the extent to which detrital zircons provide meaningful
703 age constraints depends on: (1) the extent to which autocrystic (syn-eruptive) zircon is present, and
704 (2) the time lag between the zircon crystallisation in the original magma chamber and final
705 deposition in the upper Stormberg Group (e.g., Spencer et al., 2016; Andersen et al., 2019; Gehrels
706 et al., 2019; Herriott et al., 2019; Rossignol et al. 2019). Given that both assumptions cannot be
707 independently constrained, we assume that all zircon is recycled and that MDA calculations provide
708 only a ***maximum*** constraint on the TDA (i.e., the TDA is younger or equal to the MDA). By integrating
709 MDA calculations with existing age constraints from bio-, litho-, and magnetostratigraphic
710 considerations, we show that, in many cases, the youngest detrital zircons provide meaningful age
711 constraints on the age of the upper Stormberg Group. In the following sections, we discuss the
712 implications of the new detrital zircon U-Pb ages for the geological history of the TJB-bearing Elliot
713 Formation in southern Africa from various from litho-, magneto- and biostratigraphic aspects.

714

715 **5.2 New radioisotopic dates and basin evolution**

716 **5.2.1 Lithostratigraphic considerations**

717 Based on our new geochronological dataset, obtained from U-Pb radioisotopic dates of detrital
718 zircons in the Elliot and Clarens formations (Figs. 1, 2, 4), the upper Stormberg Group probably spans
719 ~40 Ma, and we infer that this represents a sedimentation record from the middle Norian to early
720 Toarcian. In particular, the TJB-bearing Elliot Formation represents a ~30-million-year-long
721 depositional episode (from ~220 to ~190 Ma ago), of which the lEF and uEF account for ~20 and ~10
722 Ma, respectively.

723 These new age-constraints help us understand the resolution and completeness of the geological
724 history captured in the late stages of MKB evolution. The completeness of the depositional record is
725 variable across the MKB, as evidenced by the fact that the Elliot Formation, which was deposited in
726 ~30 million years, is ~500-m-thick in the south and less than 30-m-thick in the north. Assuming that

the unit's stratigraphic contacts are isochronous across the MKB, the ~30 Ma worth of rock record of the Elliot Formation can imply that this unit: (1) was deposited under low sediment preservation conditions (i.e., accumulation rates of ~1.5-27.5 m/Ma), (2) contains cryptic stratigraphic gaps, which are possibly long but rarer in the south, and short but more abundant in the north of the basin, and (3) is separated from the underlying Carnian Molteno Formation by a regional stratigraphic gap of ~6–7 Ma. In foreland basins, low sediment preservation conditions are normally favourable for mature paleosol development (e.g., DeCelles, 2012; Miall, 2016), whereas regional unconformities are typically associated with flexural tectonics driven largely by mountain building events (e.g., Catuneanu et al., 1998; Catuneanu, 2004; Bordy et al., 2004a, 2005). Moreover, the newly obtained dates also suggest that: (1) the relative resolution of the rock record is higher in the uEF compared to the lEF (Fig. 1c); and (2) the overall resolution of the Elliot rock record is modest to very low, especially in the northern part of the basin, where the thickness of the Elliot Formation is rarely >100 m.

Our radioisotopic age estimates are an important critical test of previous assessments based on relative chronostratigraphy. Nevertheless, they largely uphold those previous assertions, albeit with more nuance. While the results currently lack the spatial resolution required to precisely identify the position of the TJB at the sampling sites and for the entire basin, both vertically and laterally, these new results nonetheless support previous proposals that the TJB is close to the geological transition from lEF to uEF facies, and lay the foundation for quantifying the vertical distance between these key chrono- and lithostratigraphic boundaries (Fig. 3).

Determining the position of the TJB relative to this major stratigraphic contact will require much denser sampling of radioisotopic ages in multiple vertical sections throughout the basin. In addition to maximum depositional ages from juvenile detrital zircons, radioisotopic dating of authigenic mineral phases (e.g., feldspars, phosphates, carbonates, especially from the abundant pedogenic carbonates in the uEF) may provide useful minimum depositional ages (e.g., Wang et al. 1998; Tabor and Meyer, 2015). Such high-density geochronological sampling campaign at selected sites could also assist in reliably answering key geological questions, such as: (1) how much time is represented by the unconformity currently thought to separate the lEF from the uEF; (2) whether this stratigraphic gap is diachronous or isochronous across the basin (i.e., are there lateral changes in the size of the gap at regional and subregional scales); (3) what is the frequency and magnitude of smaller stratigraphic gaps in the lEF and uEF; and (4) what were the regional depositional dynamics in the late foreland basin history of the MKB (i.e., differential sedimentation/preservation rates from site-to-site across the basin; residence time of zircons in the dynamic fluvial setting of the Elliot

depositional episode). Establishing a higher resolution age framework in the Elliot Formation could refine the depositional history of this unit, placing its high lateral facies variability into context. It would also facilitate judicious short-range, local correlation of strata (see section 2.1, above). The latter, in turn, could also assist with robust answers to key paleobiological questions, many of which have global relevance (see section 5.4, below).

5.2.2 Sediment provenance considerations

Primary volcanic tuff layers (i.e., pyroclastics) that are suitable for robust chronostratigraphic age determinations remain elusive in the studied part of the MKB upper Stormberg succession. Such non-recycled air-fall tuffs are also commonly lacking in other Upper Triassic–Lower Jurassic continental deposits worldwide (e.g., Lucas, 2018). In the MKB, we tentatively attribute the lack of primary volcaniclastics to a combination of geological processes: (1) sediment recycling and other dynamics of continental sedimentation in foreland basins, where deep lakes, similar to those in the extensional Fundy (Canada) and Newark (USA) basins, are lacking; and (2) a potential volcanic ash fall gap in the rocks due to either a) relative inactivity or dormancy of the regional volcanic arcs in the Late Triassic to Early Jurassic or b) the site of continental deposition in the final stages of the MKB evolution was distal to major, contemporaneous volcanic eruption centres, i.e., the primary source of datable, syn-sedimentary zircon grains were located in faraway sectors of the incipiently fragmenting Pangean supercontinent (e.g., Pankhurst et al., 2006, 2014; Schiuma and Llambías, 2008; Muravchik et al., 2011; Spikings et al., 2016).

Notwithstanding the lack of primary ash fall deposits (i.e., pyroclastics), the newly acquired dataset of the detrital zircons, especially the older part of the age spectra in each sample, provides new avenues for interpreting the difference in provenance characteristics of the lEF vs uEF, and thus the depositional history of the Elliot Formation in the MKB. By tapping into this dataset, a deeper understanding of the sedimentary recycling regime and detrital zircon budget of southern Africa in the Mesozoic may be achieved, especially if this is thoughtfully combined with documented (and newly measured) sediment transport directions within the Stormberg Group (e.g., Bordy et al., 2004c, d, 2005). The most notable difference (Supplemental Table S1) between the detrital zircon populations of the lEF and uEF is that Neoproterozoic grains (~35%) are the dominant single population in the lEF, whereas Palaeozoic grains are the dominant single population in the uEF (49%), and the single Clarens Formation sample included in this study (59%). The lEF detrital zircon signature is expected from the recycling of rocks in the south from the Cape Fold Belt as well as the

792 lower Karoo rocks (Dwyka and Ecca groups; Fig. 1). The uEF detrital zircon signature, sourced from
793 the west and south and dominated by Palaeozoic grains, suggests a proximal source area of mostly
794 pre-Stormberg Karoo and Cape Fold Belt rocks (Fig. 1), with little or no input from older Precambrian
795 terranes (e.g., western Kaapvaal Craton).

796

797 **5.3 New radioisotopic dates and implications for magnetostratigraphy**

798 Using paleomagnetic and the close phylogenetic affinities of several prosauropod dinosaurs, Sciscio
799 et al. (2017a) correlated the lowermost lEF to the Los Colorados Formation (Kent et al., 2014). Given
800 the detrital zircon ages herein (Figs. 2, 4, 5), the basal magnetozone EF1r in the lEF (Fig. 2) can now
801 be more firmly tied to the LC5r magnetozone in the Los Colorados Formation. Maximum
802 depositional ages from the lowermost lEF, specifically samples PHU, HB-15, SUB (<219.6, <218.2, and
803 <216.4, respectively; Figs. 2, 4, 5), increase the credibility of tying the lEF (EF1r) to the Los Colorados
804 Formation (LC5r). By extension, these new maximum depositional ages further support correlation
805 to the radiometrically dated upper Blue Mesa and lower Sonsela members in the Chinle Formation in
806 the USA (Ramezani et al., 2011, 2014; Kent et al., 2018), although recycling of older detrital zircons in
807 these members has been reported by Gehrels et al. (2019) and Kent et al. (2019). The correlation
808 does still serve to reduce the uncertainty of the most likely basal age of the lEF to within ~3 million
809 years, and places it into the early middle Norian (i.e., within the Adamanian holochron, which has an
810 estimated age range between ~224–215 Ma in the USA; Martz and Parker, 2017). Correlation of the
811 Newark-Hartford APTS E11r–E12r, lower Chinle PF7r–PF6r and associated relative ages (~221.47 and
812 219.29 Ma, respectively; Kent et al., 2017; 2019) with the magnetozone LC5 of the Los Colorados
813 Formation (Kent et al., 2014) and therefore EF1r of the lEF complements the above statements.

814 Biostratigraphically, magnetozones EF2 and EF3 of the middle lEF (Fig. 2) can be correlated to the
815 upper third of the Los Colorados Formation (~La Esquina assemblage), with magnetozone EF2n tied
816 to LC8n (Sciscio et al., 2017a). This, in turn, links EF2 to Newark APTS E15/E16 at ~213–212 Ma (Kent
817 et al., 2017; 2018). Furthermore, correlation of the upper Chinle Formation chronostratigraphy
818 (Ramezani et al., 2011; 2014; Gehrels et al., 2019; Kent et al., 2018; 2019) to the middle lEF and the
819 upper Los Colorados Formation suggest that the EF2 may be correlated with upper Sonsela and
820 lower Petrified Forest members. This is corroborated by the middle lEF maximum depositional ages,
821 which range from <215.4 to <211.5 Ma (samples MAP, GV-14 and QSS1 Figs. 2, 4, 5). In
822 contextualising the EF2 magnetozone, EF3 is likely younger than ~210 Ma, and the lEF maximum
823 depositional ages suggest an age range between <209.6 and <207 Ma (samples HAF, LGT, LK-17) for
824 EF3. Thus, a more meaningful approximation can be made between the magnetostratigraphic and

825 depositional ages of the Petrified Forest/Painted Desert and Owl Rock members (particularly PF2r,
826 PF1r: 210.08±0.22 Ma -<207.8 Ma; Ramezani et al., 2011; 2014; Kent et al., 2018; 2019) relative to
827 the lEF EF2 and EF3 magnetozones. While the maximum depositional ages across this lEF interval
828 improve and support previous assertions of Sciscio et al. (2017a), they do not firmly constrain this
829 interval beyond <210–~205 Ma, which approximates the age of the Revueltian holochron estimated
830 by Martz and Parker (2017).

831 Elliot Formation magnetochrons EF4 –EF9n (Fig. 2) are more difficult to correlate globally based on:
832 (i) poorly constrained taxon range zone(s), (ii) lack of shared and/or diagnostic taxa with global
833 sections, and (iii) limited radioisotopic ages (see Section 5.2). The interval of the lEF represented by
834 the EF5–EF6.2n magnetozones yielded one datable sample (BH-15) with a maximum depositional
835 age of <204.9 Ma (Figs. 2, 4, 5). Based on this age and the magnetostratigraphic correlation of Sciscio
836 et al. (2017a), it is possible that lEF EF4–EF6.1r magnetozones straddle the Norian-Rhaetian
837 boundary at ~205.7 Ma (Wotzlaw et al., 2014; Maron et al., 2015), and the Newark magnetozones
838 E20r.2r, E21n and E21r.1r (and their relative ages at ~206.03 Ma, 204.65 Ma, ~204.12 Ma,
839 respectively; Kent et al., 2017). It should be noted that the lEF sample BH-15 is from a single locality
840 in the northern part of the basin, and the Newark ages are inferred from astrochronology
841 cyclostratigraphy.

842 In refining the placement of the TJB in the Elliot Formation, the current maximum depositional ages
843 for the uEF do not improve upon previous evidence from bio- and magnetostratigraphy. Sciscio et al.
844 (2017a) considered it plausible that the TJB may lie within the lower uEF, either within the normal
845 polarity chron EF6.2n or higher in the Elliot magnetostratigraphic composite sequence (i.e., within
846 EF7n; Fig. 2). The Upper Triassic-Lower Jurassic Moenave Formation was previously correlated with
847 the Elliot EF4–EF8 magnetozones based on bio- and magnetostratigraphy, and suggests an Early
848 Jurassic age for the EF7 magnetozone (EF7 = M3 magnetozone; Donohoo-Hurley et al., 2010;
849 Whiteside et al., 2011; Kirkland et al., 2014; Martz and Parker, 2017). Magnetozones EF5–EF6 have
850 not been sampled for detrital zircon-bearing samples in this study, and therefore the radioscopic age
851 of this interval remains uncertain. However, because of the occurrence of *Protosuchus* in the lower-
852 middle uEF (Dollman et al., 2017) shared with the lower Dinosaur Canyon Member (Moenave
853 Formation, USA; Suarez et al., 2017) and the Rhaetian McCoy Brook Formation (Nova Scotia,
854 Canada) could suggest that magnetozones EF5–EF6 may be latest Triassic in age, could straddle the
855 ETE, and be a reflection of the Apachean holochron (Martz and Parker, 2017).Thus, the first lower
856 Jurassic rocks of the Elliot Formation may be, potentially, within the EF7 magnetozone, and
857 therefore above the lEF/uEF boundary. However, this correlation is only weakly supported by a

858 single uEF sample (MAF) with a maximum depositional age of <201 Ma (Figs. 2, 4, 5). The pattern
859 and number of the polarity pairs in the uppermost uEF (EF7, EF8 and EF9n; Fig. 2) are not distinctive
860 enough for firm magnetostratigraphic correlations to other basins. Based on biostratigraphic
861 argument alone, Sciscio et al. (2017a) tied these magnetochrons to the Hartford H24r–H27 and the
862 St Audrie's Bay/East Quantoxhead composite AQ1r–AQ3r providing a Hettangian-Sinemurian age for
863 the upper half of the uEF. The new maximum depositional ages in this study do not assist in
864 validating this correlation, because of the limited number of productive detrital zircon-bearing
865 samples in the uEF (e.g., Q6: <191.9 Ma; LEP: <197.3 Ma, LMO: <199.9 Ma, MAF: <201 Ma; Figs. 2, 4,
866 5).

867

868 **5.4. New radioisotopic dates and implications for biostratigraphy**

869 **5.4.1 Biostratigraphic discussion**

870 The striking differences in tetrapod diversity between the uEF and lEF have long been noted but
871 have been relatively understudied. The geospatial studies undertaken here show that species-area
872 effects (Close et al., 2017) are a poor explanatory model for this difference in diversity, as the
873 geographic spread of lEF and uEF localities is nearly identical (Fig. 7). Sampling intensity may provide
874 a partial explanation, because the uEF has many more collections records than the lEF. Our database
875 currently contains 128 generically-determined records of lEF vertebrate body fossils, of which 42
876 have precise stratigraphic occurrence data, compared to 618 from the uEF (131 with precise
877 stratigraphic data). In the case of sauropodomorphs, a number of well-provenanced records in the
878 lEF are confounded by taxonomic uncertainty, and continued revision of lEF taxa will undoubtedly
879 improve our knowledge of the stratigraphic distributions of those dinosaurs. However, a sufficient
880 sample exists in the lEF to infer that theropod and ornithischian dinosaurs, as well as
881 crocodylomorphs, later-branching cynodonts, and turtles must have been rare components of
882 Norian-Rhaetian ecosystems in the MKB. This contrasts with the presence and abundance of these
883 groups in the uEF, and is suggestive of a marked faunal change during the Triassic–Jurassic
884 transition.

885 Our chronostratigraphic data show that the thicker lEF represents a longer period of time than the
886 thinner uEF (Fig. 1, 2, 4; see section 5.1), meaning that it had longer periods of non-deposition or
887 more frequent/longer periods of erosion. This likely has the effect of compressing the vertical range
888 of lEF taxa, confounding our efforts to establish meaningful biozonation. However, recent
889 biostratigraphic investigations (Viglietti et al., in press a) suggest that lEF taxa, particularly

Scalenodontoides, have a fairly wide stratigraphic distribution at least in the lower parts of the lEF, especially in the southern part of the basin (Fig. 7). This may reflect heterogeneity in depositional rates or in basinal subsidence patterns, or possibly an abnormally long duration of that genus. Targeted future collection efforts are necessary to test these hypotheses. In addition, the strong thickness variation of the lEF (see section 5.1; Bordy et al., 2004a, b, d; Bordy and Eriksson, 2015) may indicate that significant parts of the section are missing in different portions of the basin, providing fewer options to sample the entire lEF record for its tetrapod diversity.

5.4.2 Taxon sampling in the Norian–Rhaetian lEF

Our new age assessment of the Elliot and Clarens formations provides more robust temporal correlations with increasingly well-dated vertebrate faunas in the Western Hemisphere (e.g., Langer et al., 2018). In particular, we can more confidently state that the lEF overlaps in time with the well-studied faunas of the Chinle and Los Colorados formations, potentially including those from famous localities like the *Placerias* and Hayden Quarries and the La Esquina fauna.

Given that we can now confirm a Late Triassic (Norian–Rhaetian) age for the lEF, it is surprising that this unit has not yielded body fossils of the many diverse terrestrial tetrapod taxa present in other Late Triassic faunas worldwide. Representatives of small-bodied lineages that are known from Late Triassic deposits globally are absent, including mammaliaforms, rhynchocephalians, drepanosauromorphs, recumbirostrans, and pterosaurs. These absences are most likely explained by taphonomic or collector biases, which are currently uncharacterised and unexplained. However, it is unlikely that small-bodied vertebrates were actually absent from the fauna. Absences of larger-bodied groups that are widespread in other Late Triassic assemblages are more likely to reflect genuine absence, or rarity, including those from phytosaurs and several pseudosuchian lineages (such as poposauroids; see review in Knoll, 2004).

In the case of the aquatic phytosaurs, it had been suggested that their absence from southern Africa might be due to a clade-specific paleotropical preference, as all known localities were situated between ~30°N and ~30°S (Olsen and Galton, 1984; Shubin and Sues, 1991). However, discoveries of phytosaur material in the Baltic region of Europe (approximately 45° N during the Late Triassic: Brusatte et al., 2013) and in the Tashinga Formation of the Mid-Zambezi Basin, Zimbabwe (paleolatitude of approximately 40°S: Barrett et al., 2020) demonstrate conclusively that they were not constrained to the paleotropics. Although phytosaurs would have been confined to regions with perennial lakes or rivers, placing limits on their geographic range (Buffetaut, 1993), lEF

paleoenvironments were seasonally wet and supported large, permanent rivers (e.g., Smith et al., 1993; Bordy et al., 2004b, d), so their absence from the MKB remains unexplained. Interestingly, phytosaurs are also absent from the La Esquina fauna of the Los Colorados Formation.

A general explanation for the scarcity of pseudosuchians in the Elliot Formation might relate to latitudinal temperature gradients. This group, which includes extant crocodylians, has well-defined pattern of high abundance and diversity at low latitudes, and low abundance or absence at high latitudes, and has done since its origin in the Triassic (Markwick, 1998; Mannion et al., 2015). The MKB represents a relatively high paleolatitude assemblage at approximately 50° south, and this potentially explains both the relatively low abundance of pseudosuchians in the lEF, and the under-representation of pseudosuchian clades (other than crocodylomorphs). Nevertheless, this does not provide a good explanation of the abundance of crocodylomorphs in the uEF.

Until recently, dicynodont synapsids were considered to be absent from the lEF fauna (although possible trackways had been reported: Ellenberger, 1955, 1970, 1972; Ellenberger and Ellenberger, 1958; Bordy et al., 2017b), but their presence has now been demonstrated with the description of *Pentasaurus*, which also records the first known association of large-bodied dicynodonts with sauropodomorph dinosaurs from anywhere in the world (Kammerer, 2018). This occurrence provides additional evidence that placeriine dicynodonts had a Pangean distribution (Kammerer, 2018), contrary to earlier paleobiogeographic hypotheses (Kammerer et al., 2013).

5.4.3 Implications for the early evolution of Dinosauria

Revisions to the stratigraphy and age of key upper Stormberg Group vertebrate localities have major implications for our understanding of early dinosaur evolution, and particularly for understanding the diversification of Ornithischia. The early ornithischian dinosaur *Eocursor* was originally reported as from the lEF and thus of Late Triassic (Norian) age (Butler et al., 2007). Late Triassic ornithischian material has been considered to be very rare (Irmis et al., 2007) and this taxon was therefore important in calibrating divergence times within ornithischian phylogeny and in elucidating the nature of the early ornithischian *bauplan*. However, more recent work at the *Eocursor* type locality demonstrated that this material pertains to the uEF and is more likely earliest Jurassic in age (Olsen et al., 2010; McPhee et al., 2017). This revision, alongside stratigraphic and taxonomic revisions of other purported Late Triassic ornithischians, has now removed all known evidence for Late Triassic ornithischians from the global record (e.g. Irmis et al., 2007; Olsen et al., 2010; Irmis, 2011; Agnolín and Rozadilla, 2017; Baron et al., 2017a, b; Baron, 2019). This leaves an extensive ghost lineage

between the earliest confirmed ornithischians from the earliest Jurassic and their Late Triassic sister-group (either Theropoda or Saurischia; compare phylogenies of Baron et al., 2017b; Langer et al., 2017), which suggests that their early history took place in a currently unsampled area. Alternatively, this 'ornithischian gap' might represent a genuine absence that could indicate a relatively late derivation of ornithischians from within Theropoda (Padian, 2013; Baron, 2019), although this idea has not gained wide acceptance. Nevertheless, the uEF currently provides the best available window on early ornithischian evolution, possessing not only a diversity of taxa from across the tree (*Abrictosaurus*, *Eocursor*, *Heterodontosaurus*, *Lesothosaurus*, *Lycorhinus*), but an abundance of material for functional and paleoecological, as well as phylogenetic, analysis (e.g., Butler, 2005, 2010; Butler et al., 2007, 2008; Knoll, 2008; Knoll et al., 2010; Maidment and Barrett, 2011; Porro et al., 2010, 2015; Norman et al., 2011; Sereno, 2012; Galton, 2014; Barrett et al., 2016; Baron et al., 2017a, b; Sciscio et al., 2017c). The presence of a diverse ornithischian fauna in the uEF coincides with their widespread appearance in the global fossil record at this time (e.g., Irmis, 2011; Barrett et al., 2014; Raven et al., 2019; earliest Jurassic of China, Venezuela, the UK, and USA) and clear evidence of phenotypic divergence in body size, stance, and dental morphology (Benson et al., 2014; Benson, 2018). Taken together, these observations demonstrate that ornithischians radiated rapidly in the wake of the ETME.

Our results also enhance the understanding of the early evolution of sauropodomorph dinosaurs. Abundant fossil discoveries from the Elliot Formation have been central to the development of knowledge on early sauropodomorph evolution, and complement the rich record found elsewhere, particularly that from South America. Sauropodomorphs are by far the dominant vertebrate taxa in our collection records for the Norian–Rhaetian lEF (Fig. 8), echoing their relative abundances in the penecontemporaneous and latitudinally nearly equivalent Los Colorados Formation of South America (Martinez et al., 2015). During this time, sauropodomorphs underwent key morphological transitions, including the evolution of giant body size (Apaldetti et al., 2018) and the first instances of quadrupedalism (McPhee et al., 2018) and much of our understanding of these transitions results from the systematic study of the uEF body fossil record (e.g., Huxley, 1867; Haughton, 1924; Galton and Van Heerden, 1985; Yates and Kitching, 2003; Bonnan and Yates, 2007; Yates 2007b; Yates et al., 2010; McPhee et al., 2015, 2017, 2018). Body fossil specimens of sauropodomorphs from the lEF are generally less complete, and have yielded fewer direct insights into sauropodomorph evolution. For example, although limb proportions within the problematic *Plateosauravus* syntype (Haughton, 1924; Yates, 2003; McPhee et al., 2017) are suggestive of a quadrupedal locomotor habit for that taxon, unequivocally quadrupedal sauropodomorphs have yet to be identified from the lEF—despite their presence in Norian deposits of South America (*Riojasaurus*, Bonaparte, 1969; *Lessemsaurus*

and *Ingentia*, Apaldetti et al., 2018). Nonetheless, quadrupedal trackways (i.e., *Paratetrasauropus seakensis*, *Sauropodopus antiquus*, ?*Lavinipes jaquesi, Tetrasauropos unguiferus,* Ellenberger, 1970, 1972; D'Orazi Porchetti and Nicosia, 2007) are common in the lEF (fig. 2). Some of these trackways are attributed to quadrupedal sauropodomorphs, and are present within the first 15 m of the lEF (e.g., at our PHU sample site), and continue throughout that section (for example, at our MAP and HAF sample sites with MDAs 215.4 and 209.6 Ma, respectively; Figs. 4, 5). Moreover, some quadrupedal trackways (e.g., ?*Lavinipes jaquesi* - D'Orazi Porchetti and Nicosia, 2007) occur alongside the bipedal sauropodomorph trackway *Pseudotetrasauropous bipedoida*, Ellenberger, 1970, 1972; D'Orazi Porchetti and Nicosia, 2007) at our PHU sample site (Fig. 5), which has a MDA of 219.6 Ma. Therefore, we confidently infer the presence of quadrupedal sauropodomorphs in southern Africa by between ~220 and ~216 Ma. The first known multi-tonne Elliot sauropodomorphs only appear in the lower part of the uEF (*Ledumahadi*; McPhee et al 2018), postdating their first appearance in South America (Apaldetti et al., 2018). However, undescribed specimens of lEF sauropodomorphs in the South African collections record are of enormous size. Future research will likely show that both gigantic body size and quadrupedalism appeared at similar times in sauropodomorphs of the Norian of South America and southern Africa.

Mass accumulations of vertebrate fossil material have great potential to improve our knowledge of lEF faunas, especially those in the middle Norian. To-date, two major bone beds have been documented from the lower lEF, both occurring within 50 m of the lower contact of the unit. The first one, containing abundant sauropodomorph remains, was discovered in the 1950s at Maphutseng (Lesotho) (e.g., Ellenberger, 1955; Ellenberger and Ginsburg, 1966), and is located <20 m below our sample MAP (with an MDA of 215.4 MA; Figs. 4, 5). The second, found <20 km south of the Maphutseng site, is a recent discovery made by the local community near Qhemegha, a village in Eastern Cape Province, South Africa and is a multi-taxic assemblage including dinosaurs, dicynodonts, cynodonts, and possibly other taxa (JNC, PMB, RBJB, PAV, LS, EMB, unpublished results). Moreover, with one exception, all other significant lEF sauropodomorph taxa that were provenanced by McPhee et al. (2017; see their fig. 5) occur within the first ~50 m of the lEF. Considering the MDAs of strata from adjacent beds in the lEF, the two major lEF bone beds and other sauropodomorph-bearing strata in the lowermost lEF appear to have formed in the middle Norian (i.e., between ~216 and ~220 Ma), in the first 6–7 Ma after the end of the Carnian (Fig. 2).

6. Concluding remarks

The increasing sophistication (i.e., accuracy, precision) and affordability of modern dating techniques, combined with more systematic and higher density sampling efforts, will profoundly improve our understanding of the geological history of the upper Stormberg Group, a key Mesozoic terrestrial succession in the upper Karoo Supergroup of South Africa. In turn, this will increase its utility for decoding not only southern Pangean paleogeographic and ecological changes during the final stages of MKB development, but will also enhance its impact on studies of the ETME and ensuing global biodiversity changes.

Our study, which contains the first-ever and long-overdue radioisotopic assessment of the upper Stormberg Group, provides a solid initial framework for these future efforts. However, some important questions remain unanswered at this time, such as the length of the depositional hiatus between the lEF and the uEF and the stratigraphic position of the TJB and ETME. This is largely due to our relatively low number of analysed samples and applied radioisotopic methods, which were dictated by the rock types suitable for age dating and resources available to us as a group of multidisciplinary researchers, mostly based in the Global South. Nonetheless, our basin-wide study of the upper Stormberg Group gives a clear exposition of the status quo, whilst also substantially advances knowledge on the age, litho-, magneto- and biostratigraphy of this important unit. Future efforts must, therefore, focus on obtaining high-precision dates for stratigraphic sections that traverse the lEF–uEF boundary, using an intensive, densely spaced sampling regime and high-precision geochronological methods like CA-ID-TIMS. Ideally, these focus areas should be in places with abundant vertebrate fossils.

By expanding our chronostratigraphic research to potentially correlatable continental successions in southern Africa (e.g., the mid-Zambezi Basin), we will gain a better understanding of geographic controls on Triassic–Jurassic biodiversity in southern Africa. Indeed, work in that area is already underway (Viglietti et al., 2018b; Barrett et al., 2020), but more comprehensive surveys, with integrated sedimentology, biostratigraphy, magnetostratigraphy, and absolute dating methods, are needed of all upper Karoo units across southern Africa.

Finally, by integrating stable isotope geochemistry in this research (e.g., C-isotope excursions), we can potentially link major climatic changes with faunal differences on an absolute timescale – and in doing so help set a world standard for understanding landscape changes and basin development in southwestern Gondwana during the Late Triassic and Early Jurassic.

Acknowledgements

We would like to extend our sincere gratitude to Akhil Rampersadh, Maposholi Mokhethi, Howard Head, Robert Muir, Mhairi Reid, and T'Nielle Haupt who assisted us during geological fieldwork. Staff at the U-(Th)-Pb Geochronology Division in the Central Analytical Facilities of Stellenbosch University are acknowledged for guidance with detrital zircon data processing and reduction. We thank Barry Schaulis for assistance with laser ablation at the University of Arkansas TRAIL facility. Members of various field parties assisting with paleontological field work in South Africa, especially Kathleen Dollman, Casey Staunton, Katherine Clayton, Simon Wills and Matt Baron, are also acknowledged. Bernhard Zipfel, Sifelani Jirah, Zaituna Skosan, Claire Browning, Elize Butler, Jennifer Botha-Brink, Rose Prevec, William J. de Klerk, Heidi Fourie provided access to specimens and specimen records in their care in South Africa. We also thank staff at the London Natural History Museum, and Muséum National d'Histoire Naturelle Paris, and Naturhistorisches Museum Wien Vienna for assistance with the respective specimen records.

Funding:

This work was supported by the National Research Foundation (NRF) of South Africa Competitive Programme for Rated Researches (CPRR) and African Origins Programme (AOP) [grant numbers 93544, 113394, 98825 to EMB; 98906, 98800 and 118794 to JNC]; DST-NRF Centre of Excellence in Palaeosciences [COE PAL 2015, 2019 to EB; COE PAL 2015–2018 to JNC], NRF Incentive funding to EB and JNC; Palaeontological Scientific Trust (PAST) grants (2013–2015, 2017) to JNC, and the National Science Foundation (NSF) Division of Earth Sciences (EAR) Sedimentary Geology and Paleobiology (SGP) program (award #1761576 to CAS and GRS). During the study, MA and LS were recipients of postgraduate and postdoctoral funding, respectively, from the DST-NRF COE in PAL. ZR's postgraduate funding was from NRF (grant-holder linked bursary via EMB's 93544 grant) and from the post-graduate degree support grant of PAST (2016-2018). LS also acknowledges the Claude Leon Foundation Fellowship for postdoctoral funding. PMB acknowledges support from the Royal Society of London, the Earth Sciences Departmental Investment Fund (Natural History Museum, London), and NERC Facilities Grant IP-1607-1115.

The funders had no role in study design, data collection and analysis, decision to publish, or preparation of the manuscript. Opinions expressed and conclusions arrived at are those of the authors and are not necessarily to be attributed to the CoE in Palaeosciences, NRF, PAST or any other sponsor. The authors have declared that no competing interests exist.

Declarations of interest: none

Data availability

South African Heritage regulations stipulate that the biostratigraphic database must reside with a collections manager or curator. The database used in this contribution is available for all bonafide requests by emailing either bernhard.zipfel@wits.ac.za or sifelani.jirah@wits.ac.za, or the current University Curator of Collections at the University of the Witwatersrand.

All other datasets* mentioned as Supplementary Materials in the text of this article can be found at http://dx.doi.org/10.6084/m9.figshare.9730100, an open-source online data repository hosted at Figshare (Bordy et al., 2019).

[dataset] Bordy et al, Dating of the upper Stormberg Group: Datasets and Supplementary Materials, 2019, Figshare, v1, https://figshare.com/s/72ce7f31f47c8159f02d * (DOI: 10.6084/m9.figshare.9730100 - this DOI will be public upon the acceptance of the paper).

*The available data on Figshare include:

(1) Supplemental Text 1 – detailed information on the geochronological procedure (additional methods), geochronological results for each sample, and the key to animal and track outlines in Figure 2 (MS Word text file);

(2) Supplemental Table S1 – complete data set of geochronological measurements for each sample and standards (MS Excel data file);

(3) Supplemental Figure S1 – illustrations, for each sample, of the relative-age-probability plots (or probability density plots; PDP), concordia diagrams, and Isoplot of weighted mean dates with 2σ internal error bars.

References

1. Abdala, F. and Gaetano, L.C., 2018. The Late Triassic record of cynodonts: time of innovations in the mammalian lineage. In *The Late Triassic world* (pp. 407–445). Springer, Cham.
2. Abdala, F., Damiani, R., Yates, A. and Neveling, J., 2007. A non-mammaliaform cynodont from the Upper Triassic of South Africa: a therapsid Lazarus taxon. *Palaeontologia africana*, *42*, pp.17–23.
3. Abrahams, M., Bordy, E.M., Sciscio, L. and Knoll, F., 2017. Scampering, trotting, walking tridactyl bipedal dinosaurs in southern Africa: ichnological account of a Lower Jurassic palaeosurface (upper Elliot Formation, Roma Valley) in Lesotho. *Historical Biology*, 29(7), pp.958–975.
4. Agnolín, F.L. and Rozadilla, S., 2018. Phylogenetic reassessment of *Pisanosaurus mertii* Casamiquela, 1967, a basal dinosauriform from the Late Triassic of Argentina. *Journal of Systematic Palaeontology*, *16*(10), pp.853–879.
5. Andersen, T., Elburg, M. and Cawthorn-Blazeby, A., 2016. U–Pb and Lu–Hf zircon data in young sediments reflect sedimentary recycling in eastern South Africa. *Journal of the Geological Society*, *173*(2), pp.337–351. doi:10.1144/jgs2015-006.

6. Andersen, T., Elburg, M.A. and Magwaza, B.N., 2019. Sources of bias in detrital zircon geochronology: Discordance, concealed lead loss and common lead correction. E*arth-Science Reviews, 197*, p.102899.
7. Anderson, H.M. and Anderson, J.M., 1970. A preliminary review of the biostratigraphy of the uppermost Permian, Triassic and lowermost Jurassic of Gondwanaland. *Palaeontologia africana*, *13,* pp.1–22.
8. Anderson, J.M., Anderson, H.M. and Cruickshank, A.R., 1998. Late Triassic ecosystems of the Molteno/Lower Elliot biome of southern Africa. *Palaeontology*, *41*(3), pp.387–421.
9. Apaldetti, C., Martínez, R. N., Cerda, I. A., Pol, D. & Alcober, O., 2018. An early trend towards gigantism in Triassic sauropodomorph dinosaurs. *Nature Ecology & Evolution*, 2, 1227–1232.
10. Attridge, J., 1963. The Upper Triassic Karroo deposits and fauna of southern Rhodesia. *South African Journal of Science*, *59*(5), pp.242–247.
11. Baron, M.G., 2019. *Pisanosaurus mertii* and the Triassic ornithischian crisis: could phylogeny offer a solution? *Historical Biology*, 31, pp.967–981. https://doi.org/10.1080/08912963.2017.1410705
12. Baron, M.G., Norman, D.B. and Barrett, P.M., 2016. Postcranial anatomy of *Lesothosaurus diagnosticus* (Dinosauria: Ornithischia) from the Lower Jurassic of southern Africa: implications for basal ornithischian taxonomy and systematics. *Zoological Journal of the Linnean Society*, *179*(1), pp.125–168. https://doi.org/10.1111/zoj.12434.
13. Baron, M.G., Norman, D.B. and Barrett, P.M., 2017a. A new hypothesis of dinosaur relationships and early dinosaur evolution. *Nature*, *543*(7646), p.501. doi: 10.1038/nature21700.
14. Baron, M.G., Norman, D.B. and Barrett, P.M., 2017b. Untangling the dinosaur family tree Reply. *Nature*, *551*(7678), pp.E4–E5. doi:10.1038/nature24012.
15. Barrett, P.M., Butler, R.J., Mundil, R., Scheyer, T.M., Irmis, R.B. and Sánchez-Villagra, M.R., 2014. A palaeoequatorial ornithischian and new constraints on early dinosaur diversification. *Proceedings of the Royal Society B: Biological Sciences*, *281*(1791), p.20141147. https://doi.org/10.1098/rspb.2014.1147
16. Barrett, P.M., Butler, R.J., Yates, A.M., Baron, M.G. and Choiniere, J.N., 2016. New specimens of the basal ornithischian dinosaur *Lesothosaurus diagnosticus* Galton, 1978 from the Early Jurassic of South Africa. *Palaeontologia africana*, *50,* pp.48–63.
17. Barrett, P.M., Chapelle, K.E., Staunton, C.K., Botha, J. and Choiniere, J.N., 2019. Postcranial osteology of the neotype specimen of *Massospondylus carinatus* Owen, 1854 (Dinosauria: Sauropodomorpha) from the upper Elliot formation of South Africa. *Palaeontologia africana*, *53,* pp.114–178.
18. Barrett, P.M., Sciscio, L., Viglietti, P.A., Broderick, T.J., Suarez, C.A., Sharman, G.A., Jones, A.S., Munyikwa, D., Edwards, S.F., Chapelle, K.E.J., Dollman, K.N., Zondo, M. and Choiniere, J.N. 2020. The age of the Tashinga Formation (Karoo Supergroup) in the Mid-Zambezi Basin, Zimbabwe and the first phytosaur from sub-Saharan Africa. *Gondwana Research*, *81*, pp.445–460.
19. Benson, R.B.J. 2018. Dinosaur macroevolution and macroecology. *Annual Reviews of Ecology, Evolution and Systematics*, *49*, 379–408.
20. Benson, R.B.J., Campione, N.E., Carrano, M.T., Mannion, P.D., Sullivan, C., Upchurch, P. and Evans, D.C. 2014. Rates of dinosaur body mass evolution indicate 170 million years of sustained ecological innovation on the avian stem lineage. *PLOS Biology*, *12*(5), e1001853.
21. Beukes, N.J., 1970. Stratigraphy and sedimentology of the Cave Sandstone stage, Karoo System. In: S.H. Haughton (Editor), *Proceedings 2nd IUGS Symposium on Gondwana Stratigraphy and Palaeontology* (pp. 321–341). Pretoria: CSIR.
22. Black, L.P., Kamo, S.L., Allen, C.M., Davis, D.W., Aleinikoff, J.N., Valley, J.W., Mundil, R., Campbell, I.H., Korsch, R.J., Williams, I.S. and Foudoulis, C., 2004. Improved 206Pb/238U microprobe geochronology by the monitoring of a trace-element-related matrix effect; SHRIMP, ID–TIMS, ELA–ICP–MS and oxygen isotope documentation for a series of zircon standards. *Chemical Geology*, 205(1-2), pp.115–140.
23. Blackburn, T.J., Olsen, P.E., Bowring, S.A., McLean, N.M., Kent, D.V., Puffer, J., McHone, G., Rasbury, E.T. and Et-Touhami, M., 2013. Zircon U-Pb geochronology links the end-Triassic extinction with the Central Atlantic Magmatic Province. *Science*, *340*(6135), pp.941–945.
24. Blewett, S.C. and Phillips, D., 2016. An overview of Cape Fold Belt Geochronology: implications for sediment provenance and the timing of Orogenesis. In *Origin and Evolution of the Cape Mountains and Karoo Basin* (pp.45–55). Springer, Verlag. doi:10.1007/978-3-319-40859-0_5
25. Blewett, S.C., Phillips, D. and Matchan, E.L., 2019. Provenance of Cape Supergroup sediments and timing of Cape Fold Belt orogenesis: Constraints from high-precision 40Ar/39Ar dating of muscovite. *Gondwana Research*, *70*, pp.201–221. https://doi.org/10.1016/j.gr.2019.01.009.
26. Bonaparte, J.F. 1969. Dos nuevas "faunas" de reptiles Triásicos de Argentina. *Ameghiniana*, *10(1)*, 89–102.

27. Bonnan, M.F. and Yates, A.M. 2007. A new description of the forelimb of the basal sauropodomorph *Melanorosaurus*: implications for the evolution of pronation, manus shape and quadrupedalism in sauropod dinosaurs. *Special Papers in Palaeontology, 77*, 157–168.
28. Bond, G., 1973. The Palaeontology of Rhodesia. *Rhodesia Geological Survey Bulletin, 70*, pp. 1–121.
29. Bordy, E.M., Hancox, P.J. and Rubidge, B.S., 2004a. Basin development during the deposition of the Elliot Formation (Late Triassic - Early Jurassic), Karoo Supergroup, South Africa. S*outh African Journal of Geology, 107,* 395–410.
30. Bordy, E.M., Hancox, P.J. and Rubidge, B.S., 2004b. Fluvial style variations in the Late Triassic - Early Jurassic Elliot Formation, main Karoo Basin, South Africa. *Journal of African Earth Sciences, 38*, 383–400.
31. Bordy, E.M., Hancox, P.J. and Rubidge, B.S., 2004c. Provenance Study of the Late Triassic – Early Jurassic Elliot Formation, main Karoo Basin, South Africa. *South African Journal of Geology, 107,* 587–602.
32. Bordy, E.M., Hancox, P.J. and Rubidge, B.S., 2004d. A description of the sedimentology and palaeontology of the Late Triassic–Early Jurassic Elliot Formation in Lesotho. *Palaeontologia africana*, *40*, pp.43–58.
33. Bordy, E.M., Hancox, P.J. and Rubidge, B.S., 2005. The contact of the Molteno and Elliot formations through the main Karoo Basin, South Africa: a second-order sequence boundary. *South African Journal of Geology, 108,* 349–362.
34. Bordy, E.M. and Eriksson, P., 2015. Lithostratigraphy of the Elliot Formation (Karoo Supergroup), South Africa. *South African Journal of Geology*, *118*(3), pp.311–316. doi: 10.2113/gssajg.118.3.311
35. Bordy, E.M., Sciscio, L., Abdala, F., McPhee, B.W. and Choiniere, J.N., 2017a. First Lower Jurassic vertebrate burrow from southern Africa (upper Elliot Formation, Karoo Basin, South Africa). *Palaeogeography, Palaeoclimatology, Palaeoecology*, 468, pp.362–372.
36. Bordy, E.M., Abrahams, M. and Sciscio, L., 2017b. The Subeng vertebrate tracks: stratigraphy, sedimentology and a digital archive of a historic Upper Triassic palaeosurface (lower Elliot Formation), Leribe, Lesotho (southern Africa). *Bollettino della Società Paleontologica Italiana*, *56*(2), pp.181–198. doi:10.4435/BSPI.2017.12.
37. Bordy, E.M. and Head, H.V., 2018. Lithostratigraphy of the Clarens Formation (Stormberg Group, Karoo Supergroup), South Africa. *South African Journal of Geology*, *121*(1), pp.119–130.
38. Bordy, E.M., Rampersadh, A., Abrahams, M., Lockley, M.G. and Head, H.V. 2020. Tracking the Pliensbachian–Toarcian Karoo firewalkers: Trackways of quadruped and biped dinosaurs and mammaliaforms. PLoS ONE 15(1): e0226847. https://doi.org/10.1371/journal.pone.0226847
39. Bristowe, A. and Raath, M.A., 2004. A juvenile coelophysoid skull from the Early Jurassic of Zimbabwe, and the synonymy of *Coelophysis* and *Syntarsus* (USA). *Palaeontologia africana 40*, pp.31–41.
40. Brusatte, S.L., Butler, R.J., Niedźwiedzki, G., Sulej, T., Bronowicz, R. and Satkūnas, J., 2013. First record of Mesozoic terrestrial vertebrates from Lithuania: phytosaurs (Diapsida: Archosauriformes) of probable Late Triassic age, with a review of phytosaur biogeography. *Geological Magazine*, *150*(1), pp.110–122.
41. Buffetaut, E., 1993. Phytosaurs in time and space. *Paleontologia Lombarda Nuova serie*, *2*, pp.39–44.
42. Butler, R.J., 2005. The 'fabrosaurid'ornithischian dinosaurs of the upper Elliot Formation (Lower Jurassic) of South Africa and Lesotho. *Zoological Journal of the Linnean Society*, *145*(2), pp.175–218.
43. Butler, R.J., 2010. The anatomy of the basal ornithischian dinosaur Eocursor parvus from the lower Elliot Formation (Late Triassic) of South Africa. *Zoological Journal of the Linnean Society*, *160*(4), pp.648–684.
44. Butler, R.J., Porro, L.B. and Norman, D.B., 2008. A juvenile skull of the primitive ornithischian dinosaur *Heterodontosaurus tucki* from the 'Stormberg' of southern Africa. *Journal of Vertebrate Paleontology*, *28*(3), pp.702–711. https://doi.org/10.1671/0272-4634(2008)28[702:AJSOTP]2.0.CO;2.
45. Butler, R.J., Smith, R.M. and Norman, D.B., 2007. A primitive ornithischian dinosaur from the Late Triassic of South Africa, and the early evolution and diversification of Ornithischia. *Proceedings of the Royal Society B: Biological Sciences*, *274*(1621), pp.2041–2046. https://doi.org/10.1098/rspb.2007.0367.
45. Catuneanu, O., 2004. Basement control on flexural profiles and the distribution of foreland facies: the Dwyka Group of the Karoo Basin, South Africa. *Geology, 32*(6), pp.517–520.
46. Catuneanu, O., Hancox, P.J. and Rubidge, B.S., 1998. Reciprocal flexural behaviour and contrasting stratigraphies: a new basin development model for the Karoo retroarc foreland system, South Africa. *Basin Research*, *10*(4), pp.417–439.
47. Chapelle, K.E. and Choiniere, J.N., 2018. A revised cranial description of *Massospondylus carinatus* Owen (Dinosauria: Sauropodomorpha) based on computed tomographic scans and a review of cranial characters for basal Sauropodomorpha. *PeerJ*, *6*, p.e4224.

48. Chapelle, K.E.J., Barrett, P.M., Botha, J., and Choiniere, J.N., 2019. *Ngwevu intloko*: a new early sauropodomorph dinosaur from the Lower Jurassic Elliot Formation of South Africa and comments on cranial ontogeny in *Massospondylus carinatus*. PeerJ 7:e7240 https://doi.org/1.7717/peerj.7240.
49. Choiniere, J.N. and Barrett, P.M., 2015. A sauropodomorph dinosaur from the ?Early Jurassic of Lusitu, Zambia. *Palaeontologia africana*, *49*, pp.42–52.
50. Citton, P., Díaz-Martínez, I., de Valais, S., and Cónsole-Gonella, C., 2018. Triassic pentadactyl tracks from the Los Menucos Group (Río Negro province, Patagonia Argentina): possible constraints on the autopodial posture of Gondwanan trackmakers. *PeerJ 6,* e5358. https://doi.org/10.7717/peerj.5358.
51. Clark, J.M., 1986. Phylogenetic relationships of the crocodylomorph archosaurs [Ph. D. dissertation]. *Chicago, Illinois: University of Chicago*.
52. Close, R.A., Benson, R.B.J., Upchurch, P. and Butler, R.J., 2017. Controlling for the species-area effect supports constrained long-term Mesozoic terrestrial vertebrate diversification. *Nature communications*, *8*, p.15381.
53. Cohen, K.M., Finney, S.C., Gibbard, P.L., and Fan, J.-X., 2013 (updated). International Chronostratigraphic Chart of the International Commission on Stratigraphy (v2018/08). *Episodes*, *36*, pp.199–204. http://www.stratigraphy.org/ICSchart/ChronostratChart2018-08.jpg.
54. Colbert, E.H., 1989. The Triassic dinosaur *Coelophysis. Museum of Northern Arizona, No. 57*, pp.1–160.
55. Cooper, M.R., 1981. The prosauropod dinosaur *Massospondylus carinatus* Owen from Zimbabwe: its biology, mode of life and phylogenetic significance. *Occasional Papers of the National Museums and Monuments Rhodesia, Series B, Natural Sciences 6*(10), pp.690–840.
56. Corfu, F., 2013. A century of U-Pb geochronology: The long quest towards concordance. *Bulletin*, *125*(1–2), pp.33–47.
57. Coutts, D.S., Matthews, W.A. and Hubbard, S.M., 2019. Assessment of widely used methods to derive depositional ages from detrital zircon populations. *Geoscience Frontiers*. https://doi.org/10.1016/j.gsf.2018.11.002
58. Crompton, A.W. and Charig, A.J., 1962. A new ornithischian from the Upper Triassic of South Africa. *Nature*, *196*(4859), p.1074.
59. Crompton, A.W. and Ellenberger, F., 1957. On a new cynodont from the Molteno Beds and the origin of the tritylodontids. *Annals of the South African Museum, 44*(1), pp.1–13.
60. Crompton, A.W. and Jenkins, F.A., 1968. Molar occlusion in Late Triassic mammals. *Biological Reviews*, *43*(4), pp.427–458.
61. de Fabrègues, C.P. and Allain, R., 2016. New material and revision of *Melanorosaurus thabanensis*, a basal sauropodomorph from the Upper Triassic of Lesotho. *PeerJ*, 4, p.e1639.
62. De Kock, M.O. and Kirschvink, J.L., 2004. Paleomagnetic constraints on the Permian-Triassic boundary in terrestrial strata of the Karoo Supergroup, South Africa: implications for causes of the end-Permian extinction event. *Gondwana Research*, *7*(1), pp.175–183.
63. De Kock, M.O., 2003. *Selected magnetostratigraphic studies in the main Karoo Basin (South Africa): implications for mass extinction events and the supercontinent of Pangea* (Masters dissertation, University of Johannesburg).
64. DeCelles, P.G., 2012. Foreland basin systems revisited: Variations in response to tectonic settings. *Tectonics of sedimentary basins: Recent advances*, pp.405–426.
65. Dickinson, W.R. and Gehrels, G.E., 2009. Use of U–Pb ages of detrital zircons to infer maximum depositional ages of strata: a test against a Colorado Plateau Mesozoic database. *Earth and Planetary Science Letters*, *288*(1-2), pp.115–125.
66. Dollman, K.N., Viglietti, P.A. and Choiniere, J.N., 2019. A new specimen of *Orthosuchus stormbergi* (Nash 1968) and a review of the distribution of Southern African Lower Jurassic crocodylomorphs. *Historical Biology, 31*(5), pp.653–664.
67. Donohoo-Hurley, L.L., Geissman, J.W. and Lucas, S.G., 2010. Magnetostratigraphy of the uppermost Triassic and lowermost Jurassic Moenave Formation, western United States: Correlation with strata in the United Kingdom, Morocco, Turkey, Italy, and eastern United States. *Geological Society of America Bulletin*, *122*(11–12), pp.2005–2019.
68. D'Orazi Porchetti, S. and Nicosia, U. 2007. Re-examination of some large early Mesozoic tetrapod footprints from the African collection of Paul Ellenberger. *Ichnos, 14,* 219-245.
69. D'Orazi Porchetti, S., Bertini, R.J. and Langer, M.C., 2017. Walking, running, hopping: analysis of gait variability and locomotor skills in *Brasilichnium elusivum* Leonardi, with inferences on trackmaker identification. *Palaeogeography, Palaeoclimatology, Palaeoecology*, *465*, pp.14–29.

70. D'Orazi Porchetti, S., Bertini, R.J. and Langer, M.C., 2018. Proposal for ichnotaxonomic allocation of therapsid footprints from the Botucatu Formation (Brazil). *Ichnos*, *25*(2-3), pp.192–207.
71. D'Orazi Porchetti, S., Mocke, H.B., Latiano, M. and Wagensommer, A., 2015. First record of *Otozoum* from Namibia. *Lethaia*, *48*(1), pp.72–82.
72. Duane, M.J. and Brown, R.W., 1992. Geochemical open-system behaviour related to fluid flow and metamorphism in the Karoo Basin. *Inversion Tectonics of the Cape Fold Belt, Karoo and Cretaceous Basins of Southern Africa. Rotterdam, AA Balkema, The Netherlands*, *127*, p.137.
73. Duncan, R.A., Hooper, P.R., Rehacek, J., Marsh, J. and Duncan, A.R., 1997. The timing and duration of the Karoo igneous event, southern Gondwana. *Journal of Geophysical Research: Solid Earth*, *102*(B8), pp.18127–18138. https://doi.org/10.1029/97JB00972.
74. Ellenberger, F. and Ginsburg, L., 1966. Le gisement de dinosauriens triasiques de Maphutseng (Basutoland) et lorigine des sauropodes. *Comptes Rendus des Seances de l 'Acadamie des Sciences Serie D*, *262*(4), pp.444–447.
75. Ellenberger, F., and Ellenberger, P., 1958. Main types of vertebrate footprints in the Stormberg beds of Basutoland (South Africa). (Preliminary note). *Compte rendu sommaire des séances de la Société Géologique de France*, pp.65–67.
76. Ellenberger, F., Ellenberger, P., Fabre, J., Ginsburg, L. and Mendrez, C., 1964. The Stormberg Series of Basutoland (South Africa). In *Reports of the 22nd International Geological Congress*, *9*, pp.320–330.
77. Ellenberger, P., 1955. Note preliminaire sur les pistes et les restes osseux de vertebres du Basutoland (Afrique-Du-Sud). *Comptes rendus des Séances de l'Academie des Sciences*, *240*(8), pp.889–891.
78. Ellenberger, P., 1970. The fossil-bearing strata associated with the earliest appearance of mammals in South Africa and their ichnology: establishment of detailed stratigraphic zones in the Stormberg of Lesotho, South Africa, Upper Triassic to Jurassic. In *Proceedings and Papers of the Second Gondwanaland Symposium on Gondwana Stratigraphy and Palaeontology. Council for Scientific & Industrial Research, Pretoria* (pp.343–370).
79. Ellenberger, P., 1972. Contribution to the classification of Triassic vertebrate trackways: types found in the Stormberg Series of South Africa (I). *Palaeo-vertebrata, Memoire Extraordinaire, Montpellier,* pp. 134.
80. Ellenberger, P., 1974. Contribution à la classification des pistes de vertébrés du Trias: les types du Stormberg d'Afrique du Sud (IIème partie: Le Stormberg superieur). Laboratoire de paléontologie des vertébrés. *Palaeo–vertebrata, Memoire Extraordinaire, Montpellier,* pp. 142.
81. Eriksson, P.G., 1986. Aeolian dune and alluvial fan deposits in the Clarens Formation of the Natal Drakensberg. *Transactions of the Geological Society of South Africa*, *89*, pp.389-394.
82. Evans, S.E. and Kermack, K.A., 1994. Assemblages of small tetrapods from the Early Jurassic of Britain. In: Fraser, N.C., and Sues, H.-D., (Eds). *In the shadow of the dinosaurs: Early Mesozoic tetrapods*, Cambridge University Press, pp.271–283.
83. Ezcurra, M.D. and Brusatte, S.L., 2011. Taxonomic and phylogenetic reassessment of the early neotheropod dinosaur *Camposaurus arizonensis* from the Late Triassic of North America. *Palaeontology*, *54*(4), pp.763–772.
84. Fraser, N.C., 1988. The osteology and relationships of *Clevosaurus* (Reptilia: Sphenodontida). *Philosophical Transactions of the Royal Society of London. B, Biological Sciences*, *321*(1204), pp.125–178.
85. Gaffney, E.S. and Kitching, J.W., 1994.The most ancient African turtle. *Nature, 369*, pp.55–58.
86. Galton, P.M., 1972. Classification and evolution of ornithopod dinosaurs. *Nature*, *239*(5373), p.464.
87. Galton, P.M., 1985. The poposaurid thecodontian *Teratosaurus suevicus v.* Meyer, plus referred specimens mostly based on prosauropod dinosaurs, from the Middle Stubensandstein (Upper Triassic) of Nordwürttemberg. *Stuttgarter Beiträge zur Naturkunde Serie B (Geologie und Paläontologie*) *116*, pp.1–29.
88. Galton, P.M., 2014. Notes on the postcranial anatomy of the heterodontosaurid dinosaur *Heterodontosaurus tucki*, a basal ornithischian from the Lower Jurassic of South Africa. *Revue de Paléobiologie*, *33*(1), pp.97–141.
89. Galton, P.M. and Van Heerden, J., 1985. Partial hindlimb of *Blikanasaurus cromptoni* n. gen. and n. sp., representing a new family of prosauropod dinosaurs from the Upper Triassic of South Africa. *Geobios*, *18*(4), pp.509–516.
90. Galton, P.M., Van Heerden, J., and Yates, A.M., 2005. Postcranial anatomy of referred specimens of the sauropodomorph dinosaur *Melanorosaurus* from the Upper Triassic of South Africa. In: V. Tidwell and K. Carpenter (eds.), Thunder-Lizards: the Sauropodomorph Dinosaurs, 1–37. Indiana University Press, Bloomington.
91. Gauffre, F.-X. 1993. The most recent Melanorosauridae (Saurischia, Prosauropoda), Lower Jurassic of Lesotho, with remarks on the prosauropod phylogeny. *Neues Jahrbuch für Geologie und Paläontologie, 11*, pp.648–654.

92. Gehrels, G., Giesler, D., Olsen, P., Kent, D., Marsh, A., Parker, W., Rasmussen, C., Mundil, R., Irmis, R., Geissman, J., and Lepre, C. , in review, 2019. LA-ICPMS U-Pb geochronology of detrital zircon grains from the Coconino, Moenkopi, and Chinle Formations in the Petrified Forest National Park (Arizona). *Geochronology Discussion*, https://doi.org/10.5194/gchron-2019-12
93. Gierliński, G. and Potemska, A., 1985. *Protosuchu*s sp. z dolnej jury północnego obrzeżenia Gór Świętokrzyskich. *Przegląd Geologiczny*, *33*(10), pp.567–570.
94. Godefroit, P. and Sigogneau-Russell, D., 1995. Cynodontes et Mammiferes primitifs du Trias Superieur, en region Lorraine et Luxembourgeoise. *Bulletin de la Société belge de Géologie*, *104*, pp.9–21.
95. Gow, C.E., 1977. Fossil vertebrate studies in Rhodesia: sphenodontid remains from the Upper Trias of Rhodesia. *Palaeontologia africana, 20*, pp.121–122.
96. Gow, C.E. and Hancox, P.J., 1993. First complete skull of the Late Triassic *Scalenodontoides* (Reptilia, Cynodontia) from southern Africa. *New Mexico Museum of Natural History and Science Bulletin, 3*, pp.161–168.
97. Gow, C.E., Kitching, J.W. and Raath, M.A., 1990. Skulls of the prosauropod dinosaur *Massospondylus carinatus* Owen in the collections of the Bernard Price Institute for Palaeontological Research. *Palaeontologia africana,* 27, pp.45–58.
98. Griffin, C.T. and Nesbitt, S.J., 2019. Does the maximum body size of theropods increase across the Triassic–Jurassic boundary? Integrating ontogeny, phylogeny, and body size. *The Anatomical Record*. DOI: 10.1002/ar.24130
99. Hälbich, I.W., Fitch, F.J. and Miller, J.A., 1983. Dating the Cape orogeny. In: Sohnge, A. P. G., and Hälbich, I. W., (Eds). Geodynamics of the Cape Fold Belt. *Special Publication of the Geological Society of South Africa, 12*, pp.149–164.
100. Hansma, J., Tohver, E., Schrank, C., Jourdan, F. and Adams, D., 2016. The timing of the Cape Orogeny: New 40Ar/39Ar age constraints on deformation and cooling of the Cape Fold Belt, South Africa. *Gondwana Research*, *32*, pp.122–137. https://doi.org/10.1016/j.gr.2015.02.005
101. Haughton, S.H., 1924. The fauna and stratigraphy of the Stormberg Series. *Annals of the South African Museum*, *12*(8), pp.323–497.
102. Herrera-Flores, J.A., Stubbs, T.L., Elsler, A. and Benton, M.J., 2018. Taxonomic reassessment of *Clevosaurus latidens* Fraser, 1993 (Lepidosauria, Rhynchocephalia) and rhynchocephalian phylogeny based on parsimony and Bayesian inference. *Journal of Paleontology*, *92*(4), pp.734–742. doi:10.1017/jpa.2017.136
103. Herriott, T.M., Crowley, J.L., Schmitz, M.D., Wartes, M.A. and Gillis, R.J., 2019. Exploring the law of detrital zircon: LA-ICP-MS and CA-TIMS geochronology of Jurassic forearc strata, Cook Inlet, Alaska, USA. Geology, 47(11), pp.1044–1048.
104. Hopson, J.A., 1984. Late Triassic traversodont cynodonts from Nova Scotia and southern Africa. *Palaeontologia africana*, 25, pp.181–201.
105. Hsiou, A. S., Nydam, R. L., Simões, T. R., Pretto, F. A., Onary, S., Martinelli, A. G., Liparini, A., Martínez, P. R. R. D. V., Soares, M. B., Schultz, C. L. & Caldwell, M. W. 2019. A New Clevosaurid from the Triassic (Carnian) of Brazil and the Rise of Sphenodontians in Gondwana. *Scientific Reports, 9*, 11821.
106. Hsiou, A.S., De França, M.A.G. and Ferigolo, J., 2015. New data on the *Clevosaurus* (Sphenodontia: Clevosauridae) from the Upper Triassic of southern Brazil. *PloS one*, *10*(9), p.e0137523. doi:10.1371/journal.pone.0137523.
107. Huang, C., 2018. Astronomical Time Scale for the Mesozoic. In: Montenari, M., (Ed.). *Cyclostratigraphy and Astrochronology*, *Stratigraphy & Timescales 3*, pp.82–150. https://doi.org/10.1016/bs.sats.2018.08.005.
108. Hunt, A.P., Lucas, S.G. and Klein, H., 2018. Late Triassic nonmarine vertebrate and invertebrate trace fossils and the pattern of the Phanerozoic record of vertebrate trace fossils. In *The Late Triassic World* (pp.447–544). Springer, Cham.
109. Hüsing, S.K., Beniest, A., van der Boon, A., Abels, H.A., Deenen, M.H.L., Ruhl, M. and Krijgsman, W., 2014. Astronomically-calibrated magnetostratigraphy of the Lower Jurassic marine successions at St. Audrie's Bay and East Quantoxhead (Hettangian–Sinemurian; Somerset, UK). *Palaeogeography, Palaeoclimatology, Palaeoecology*, *403*, pp.43–56. https://doi.org/10.1016/j.palaeo.2014.03.022.
110. Huxley, T. H., 1867. On the remains of large dinosaurian reptiles from the Stormberg Mountains, South Africa. *Quarterly Journal of the Geological Society*, *23*, pp.1–6.
111. Irmis, R.B. 2011. Evaluating hypotheses for the early diversification of dinosaurs. *Earth and Environmental Transactions of the Royal Society of Edinburgh*, *101*, 397-426.
112. Irmis, R.B., Parker, W.G., Nesbitt, S.J. and Liu, J., 2007. Early ornithischian dinosaurs: the Triassic record. *Historical Biology*, *19*(1), pp.3–22.

113. Irmis, R.B., Mundil, R., Martz, J.W. and Parker, W.G., 2011. High-resolution U–Pb ages from the Upper Triassic Chinle Formation (New Mexico, USA) support a diachronous rise of dinosaurs. *Earth and Planetary Science Letters*, *309*(3-4), pp.258–267. https://doi.org/10.1016/j.epsl.2011.07.015.
114. Johnstone, S.A., Schwartz, T.M. and Holm-Denoma, C.S., 2019. A stratigraphic approach to inferring depositional ages from detrital geochronology data. *Frontiers in Earth Science, 7*, p.57.doi: 10.3389/feart.2019.00057.
115. Kammerer, C.F., 2018. The first skeletal evidence of a dicynodont from the lower Elliot Formation of South Africa. *Palaeontologia africana, 52*, pp.102–128.
116. Kammerer, C.F., Fröbisch, J. and Angielczyk, K.D., 2013. On the validity and phylogenetic position of *Eubrachiosaurus browni*, a kannemeyeriiform dicynodont (Anomodontia) from Triassic North America. *PLOS One*, *8*(5), p.e64203. https://doi.org/10.1371/journal.pone.0064203.
117. Kent, D.V., Malnis, P.S., Colombi, C.E., Alcober, O.A. and Martínez, R.N., 2014. Age constraints on the dispersal of dinosaurs in the Late Triassic from magnetochronology of the Los Colorados Formation (Argentina). *Proceedings of the National Academy of Sciences*, *111*(22), pp.7958–7963. https://doi.org/10.1073/pnas.1402369111.
118. Kent, D.V., Olsen, P.E. and Muttoni, G., 2017. Astrochronostratigraphic polarity time scale (APTS) for the Late Triassic and Early Jurassic from continental sediments and correlation with standard marine stages. *Earth-Science Reviews*, *166*, pp.153–180. https://doi.org/10.1016/j.earscirev.2016.12.014.
119. Kent, D.V., Olsen, P.E., Rasmussen, C., Lepre, C., Mundil, R., Irmis, R.B., Gehrels, G.E., Giesler, D., Geissman, J.W. and Parker, W.G., 2018. Empirical evidence for stability of the 405-kiloyear Jupiter–Venus eccentricity cycle over hundreds of millions of years. *Proceedings of the National Academy of Sciences*, *115*(24), pp.6153–6158. doi: 10.1073/pnas.1800891115.
120. Kent, D.V., Olsen, P.E., Lepre, C., Rasmussen, C., Mundil, R., Gehrels, G.E., Giesler, D., Irmis, R.B., Geissman, J.W. and Parker, W.G., 2019. Magnetochronology of the entire Chinle Formation (Norian age) in a scientific drill core from Petrified Forest National Park (Arizona, USA) and implications for regional and global correlations in the Late Triassic. *Geochemistry, Geophysics, Geosystems*, *20*, pp.4654–4664. https://doi.org/10.1029/2019GC008474
121. Kirkland, J.I., Milner, A.R.C., Olsen, P.E. and Hargrave, J.E., 2014. The Whitmore Point Member of the Moenave Formation in its type area in Northern Arizona and its age and correlation with the section in St. George, Utah: evidence for two major lacustrine sequences. *Geology of Utah's Far South: Utah Geological Association Publication*, *43*, pp.321–356.
122. Kitching, J.W., and Raath, M.A., 1984. Fossils from the Elliot and Clarens Formations (Karoo Sequence) of the North-eastern Cape, Orange Free State and Lesotho, and a suggested biozonation based on tetrapods. *Palaeontologia africana*, *25*, pp.111–125.
123. Klein, H. and Lucas, S.G., 2010. Tetrapod footprints-their use in biostratigraphy and biochronology of the Triassic. *Geological Society, London, Special Publications*, *334*(1), pp.419–446.
124. Klein, H., Milàn, J., Clemmensen, L.B., Frobøse, N., Mateus, O., Klein, N., Adolfssen, J.S., Estrup, E.J. and Wings, O., 2016. Archosaur footprints (cf. Brachychirotherium) with unusual morphology from the Upper Triassic Fleming Fjord Formation (Norian–Rhaetian) of East Greenland. *Geological Society, London, Special Publications*, *434*(1), pp.71–85.
125. Knoll, F., 2004. Review of the tetrapod fauna of the "Lower Stormberg Group" of the main Karoo Basin (southern Africa): implication for the age of the Lower Elliot Formation. *Bulletin de la Societe géologique de France*, *175*(1), pp.73–83.
126. Knoll, F., 2005. The tetrapod fauna of the Upper Elliot and Clarens formations in the main Karoo Basin (South Africa and Lesotho). *Bulletin de la Société géologique de France*, *176*(1), pp.81–91.
127. Knoll, F., 2008. Buccal soft anatomy in *Lesothosaurus* (Dinosauria: Ornithischia). *Neues Jahrbuch für Geologie und Paläontologie-Abhandlungen*, *248*(3), pp.355-364.
128. Knoll, F., 2010. A primitive sauropodomorph from the upper Elliot Formation of Lesotho. *Geological Magazine, 147*(6), pp.814-829.
129. Knoll, F., Padian, K. and de Ricqlès, A., 2010. Ontogenetic change and adult body size of the early ornithischian dinosaur Lesothosaurus diagnosticus: implications for basal ornithischian taxonomy. *Gondwana Research*, *17*(1), pp.171–179.
130. Labandeira, C.C., Anderson, J.M. and Anderson, H.M., 2018. Expansion of arthropod herbivory in Late Triassic South Africa: The Molteno Biota, Aasvoëlberg 411 site and developmental biology of a gall. In *The Late Triassic World* (pp.623–719). Springer, Cham.
131. Lanci, L., Tohver, E., Wilson, A. and Flint, S., 2013. Upper Permian magnetic stratigraphy of the lower Beaufort Group, Karoo Basin. *Earth and Planetary Science Letters*, *375*, pp.123–134.

132. Langer, M.C., Ezcurra, M.D., Rauhut, O.W., Benton, M.J., Knoll, F., McPhee, B.W., Novas, F.E., Pol, D. and Brusatte, S.L., 2017. Untangling the dinosaur family tree. *Nature*, *551*(7678), p.E1.
133. Langer, M.C., Ramezani, J. and Da Rosa, Á.A., 2018. U-Pb age constraints on dinosaur rise from south Brazil. *Gondwana Research*, *57*, pp.133–140.
134. Langereis, C.G., Krijgsman, W., Muttoni, G. and Menning, M., 2010. Magnetostratigraphy–concepts, definitions, and applications. *Newsletters on Stratigraphy*, *43*(3), pp.207–233.
135. Lockley, M.G. and Gierlinski, G.D., 2006. Diverse vertebrate ichnofaunas containing *Anomoepus* and other unusual trace fossils from the Lower Jurassic of the western United States: implications for paleoecology palichnostratigraphy. The Triassic–Jurassic Terrestrial Transition. *New Mexico Museum of Natural History and Science Bulletin, 37*, pp.176–191.
136. Lockley, M.G., Lucas, S.G., Gaston, R., and Hunt, A.P., 2004. Ichnofaunas from the Triassic-Jurassic boundary sequences of the Gateway area, Western Colorado: implications for faunal composition and correlations with other areas. *Ichnos, 11*, pp. 89–102.
137. Lockley, M.G., Meyer, C.A. and dos Santos, V.F., 1996. *Megalosauripus, Megalosauropus* and the concept of megalosaur footprints. In *The Continental Jurassic: Symposium Volume: Museum of Northern Arizona Bulletin,* 60, pp.113–118.
138. Lockley, M.G., Lucas, S.G. and Hunt, A.P., 2006. *Eosauropus*, a new name for a Late Triassic track: further observations on the Late Triassic ichnogenus *Tetrasauropus* and related forms, with notes on the limits of interpretation. The Triassic–Jurassic Terrestrial Transition. *New Mexico Museum of Natural History and Science Bulletin, 37*, pp.192–198.
139. Lucas, S.G., 1998. Global Triassic tetrapod biostratigraphy and biochronology. *Palaeogeography, Palaeoclimatology, Palaeoecology*, *143*(4), pp.347–384.
140. Lucas, S.G., 2007. Tetrapod footprint biostratigraphy and biochronology. *Ichnos*, *14*(1-2), pp.5–38.
141. Lucas, S.G., 2018. The Late Triassic World: Earth in a Time of Transition. In: Tanner, L.H., (Ed.). *The Late Triassic World: Earth in a Time of Transition.* Cham: Springer International Publishing, pp.1–25.
142. Lucas, S.G. and Hancox, P.J., 2001. Tetrapod-based correlation of the nonmarine Upper Triassic of southern Africa. *Albertiana*, *25*, pp.5–9.
143. Luo, Z.X. and Wu, X.C., 1994. The small tetrapods of the lower Lufeng Formation, Yunnan, China. In: Fraser, N.C., and H-D., Sues, (Eds). *The Shadow of the Dinosaurs: Early Mesozoic Tetrapods*, Cambridge University Press, pp.251–270.
144. Maidment, S.C. and Barrett, P.M., 2011. The locomotor musculature of basal ornithischian dinosaurs. *Journal of Vertebrate Paleontology*, *31*(6), pp.1265–1291.
145. Mannion, P.D., Benson, R.B.J., Carrano, M.T., Tennant, J.P., Judd, J. and Butler, R.J. 2015. Climate constrains the evolutionary history and biodiversity of crocodilians. *Nature Communications*, *6*, 8438.
146. Markwick, P.J. 1998. Crocodilian diversity in space and time: the role of climate in paleoecology and its implication for understanding K/T extinctions. *Paleobiology*, *24*, 470-497.
147. Maron, M., Muttoni, G., Rigo, M., Gianolla, P. and Kent, D.V., 2018. New magnetobiostratigraphic results from the Ladinian of the Dolomites and implications for the Triassic geomagnetic polarity timescale. *Palaeogeography, Palaeoclimatology, Palaeoecology. 517*, pp.52–73. doi:10.1016/j.palaeo.2018.11.024
148. Maron, M., Rigo, M., Bertinelli, A., Katz, M.E., Godfrey, L., Zaffani, M. and Muttoni, G., 2015. Magnetostratigraphy, biostratigraphy, and chemostratigraphy of the Pignola-Abriola section: New constraints for the Norian-Rhaetian boundary. *Bulletin*, *127*(7-8), pp.962–974.
149. Marsh, A.D. and Rowe, T.B., 2018. Anatomy and systematics of the sauropodomorph *Sarahsaurus aurifontanalis* from the Early Jurassic Kayenta Formation. *PloS one*, *13*(10), p.e0204007. doi:10.1371/journal.pone.0204007
150. Marsicano, C.A., Wilson, J.A. and Smith, R.M., 2014. A temnospondyl trackway from the early mesozoic of western Gondwana and its implications for basal tetrapod locomotion. *PloS one*, *9*(8), p.e103255.
151. Martínez, R.N. and Apaldetti, C., 2017. A Late Norian—Rhaetian Coelophysid Neotheropod (Dinosauria, Saurischia) from the Quebrada Del Barro Formation, Northwestern Argentina. *Ameghiniana*, *54*(5), pp.488–506.
152. Martínez, R.N., Apaldetti, C., Correa, G., Colombi, C.E., Fernández, E., Santi Malnis, P., Praderio, A., Abelín, D., Benegas, L.G., Aguilar-Cameo, A., & Alcober, O.A., 2015. A new Late Triassic vertebrate assemblage from northwestern Argentina. *Ameghiniana* (52), pp.379–390.
153. Martz, J.W. and Parker, W.G., 2010. Revised lithostratigraphy of the Sonsela Member (Chinle Formation, Upper Triassic) in the southern part of Petrified Forest National Park, Arizona. *PLoS One*, *5*(2), p.e9329.

154. Martz, J.W. and Parker, W.G., 2017. Revised formulation of the Late Triassic Land Vertebrate "Faunachrons" of western North America: recommendations for codifying nascent systems of vertebrate biochronology. In: Zeigler, K.E., and Parker, W., (Eds.). *Terrestrial Depositional Systems: Deciphering Complexities Through Multiple Stratigraphic Methods.* Elsevier, pp.39–125. doi: 10.1016/B978-0-12-803243-5.00002-9.
155. Marzola, M., Mateus, O., Shubin, N.H. and Clemmensen, L.B., 2017. *Cyclotosaurus naraserluki*, sp. nov., a new Late Triassic cyclotosaurid (Amphibia, Temnospondyli) from the Fleming Fjord Formation of the Jameson Land Basin (East Greenland). *Journal of Vertebrate Paleontology*, *37*(2), p.e1303501.
156. Mattinson, J.M., 2005. Zircon U–Pb chemical abrasion ("CA-TIMS") method: combined annealing and multi-step partial dissolution analysis for improved precision and accuracy of zircon ages. *Chemical Geology*, *220*(1-2), pp.47–66. https://doi.org/10.1016/j.chemgeo.2005.03.011.
157. McLean, N.M., Condon, D.J., Schoene, B. and Bowring, S.A., 2015. Evaluating uncertainties in the calibration of isotopic reference materials and multi-element isotopic tracers (EARTHTIME Tracer Calibration Part II). *Geochimica et Cosmochimica Acta*, *164*, pp.481–501. https://doi.org/10.1016/j.gca.2015.02.040.
158. McPhee, B.W., Benson, R.B., Botha-Brink, J., Bordy, E.M. and Choiniere, J.N., 2018. A giant dinosaur from the earliest Jurassic of South Africa and the transition to quadrupedality in early sauropodomorphs. *Current Biology*, *28*(19), pp.3143–3151.
159. McPhee, B.W., Bonnan, M.F., Yates, A.M., Neveling, J. and Choiniere, J.N., 2015b. A new basal sauropod from the pre-Toarcian Jurassic of South Africa: evidence of niche-partitioning at the sauropodomorph–sauropod boundary?. *Scientific Reports*, *5*, p.13224.
160. McPhee, B.W., Bordy, E.M., Sciscio, L. and Choiniere, J.N., 2017. The sauropodomorph biostratigraphy of the Elliot Formation of southern Africa: Tracking the evolution of Sauropodomorpha across the Triassic–Jurassic boundary. *Acta Palaeontologica Polonica*, *62*(3), pp.441–465. doi:10.4202/app.00377.2017
161. McPhee, B.W., Choiniere, J.N., Yates, A.M. and Viglietti, P.A., 2015a. A second species of *Eucnemesaurus* Van Hoepen, 1920 (Dinosauria, Sauropodomorpha): new information on the diversity and evolution of the sauropodomorph fauna of South Africa's lower Elliot Formation (latest Triassic). *Journal of Vertebrate Paleontology*, *35*(5), p.e980504.
162. McPhee, B.W., Yates, A.M., Choiniere, J.N. and Abdala, F., 2014. The complete anatomy and phylogenetic relationships of *Antetonitrus ingenipes* (Sauropodiformes, Dinosauria): implications for the origins of Sauropoda. *Zoological Journal of the Linnean Society*, *171*(1), pp.151–205.
163. Miall, A.D., 2013. Sophisticated stratigraphy. *The web of geological sciences: Advances, impacts and interactions: Geological Society of America Special Paper*, *500*, pp.169–190.
164. Miall, A.D., 2015. Updating uniformitarianism: stratigraphy as just a set of 'frozen accidents'. *Geological Society, London, Special Publications*, *404*(1), pp.11–36.
165. Miall, A.D., 2016. The valuation of unconformities. *Earth-Science Reviews*, *163*, pp.22–71.
166. Moreau, M.G., Bucher, H., Bodergat, A.M. and Guex, J., 2002. Pliensbachian magnetostratigraphy: new data from Paris Basin (France). *Earth and Planetary Science Letters*, *203*(2), pp.755–767.
167. Moulin, M., Courtillot, V., Fluteau, F. and Valet, J.P., 2012. The "van Zijl" Jurassic geomagnetic reversal revisited. *Geochemistry, Geophysics, Geosystems*, *13*(3), Q03010. http://dx.doi.org/10.1029/2011GC003910.
168. Moulin, M., Fluteau, F., Courtillot, V., Marsh, J., Delpech, G., Quidelleur, X., Gérard, M. and Jay, A.E., 2011. An attempt to constrain the age, duration, and eruptive history of the Karoo flood basalt: Naude's Nek section (South Africa). *Journal of Geophysical Research: Solid Earth*, *116*(B7). http://dx.doi.org/10.1029/2011JB008210.
169. Moulin, M., Fluteau, F., Courtillot, V., Marsh, J., Delpech, G., Quidelleur, X. and Gérard, M., 2017. Eruptive history of the Karoo lava flows and their impact on early Jurassic environmental change. *Journal of Geophysical Research: Solid Earth*, *122*(2), pp.738–772.
170. Munyikwa, D., 1997. Faunal analysis of Karoo-aged sediments in the northern Limpopo Valley, Zimbabwe. *Arnoldia Zimbabwe*, *10*(13), pp.129–139.
171. Munyikwa, D., and Raath, M.A., 1999. Further material of the ceratosaurian dinosaur *Syntarsus* from the Elliot Formation (Early Jurassic) of South Africa. *Palaeontologia africana, 35*, pp.55–59.
172. Muravchik, M., D'Elia, L., Bilmes, A. and Franzese, J.R., 2011. Syn-eruptive/inter-eruptive relations in the syn-rift deposits of the Precuyano Cycle, Sierra de Chacaico, Neuquén Basin, Argentina. *Sedimentary Geology*, *238*(1-2), pp.132–144.
173. Norman, D.B., Crompton, A.W., Butler, R.J., Porro, L.B. and Charig, A.J., 2011. The Lower Jurassic ornithischian dinosaur *Heterodontosaurus tucki* Crompton & Charig, 1962: cranial anatomy, functional morphology, taxonomy, and relationships. *Zoological Journal of the Linnean Society*, *163*(1), pp.182–276.

174. Olsen, P.E. and Galton, P.M., 1984. A review of the reptile and amphibian assemblages from the Stormberg of southern Africa, with special emphasis on the footprints and the age of the Stormberg. *Palaeontologia africana, 25*, pp.87–110.
175. Olsen, P.E. and Sues, H.D., 1986. Correlation of continental Late Triassic and Early Jurassic sediments, and patterns of the Triassic–Jurassic tetrapod transition. *The beginning of the age of dinosaurs. Cambridge University Press, Cambridge*, pp.321–351.
176. Olsen, P.E., Kent, D.V. and Whiteside, J.H., 2010. Implications of the Newark Supergroup-based astrochronology and geomagnetic polarity time scale (Newark-APTS) for the tempo and mode of the early diversification of the Dinosauria. *Earth and Environmental Science Transactions of the Royal Society of Edinburgh*, *101*(3-4), pp.201–229. doi: 10.1017/S1755691011020032.
177. Opdyke, N.D., 1964. The paleomagnetism of some Triassic red beds from Northern Rhodesia. *Journal of Geophysical Research*, *69*(12), pp.2495–2497.
178. Otero, A., Krupandan, E., Pol, D., Chinsamy, A., and Choiniere, J.N., 2015. A new basal sauropodiform from South Africa and the phylogenetic relationships of basal sauropodomorphs. *Zoological Journal of the Linnean Society* 174, pp.589–634.
179. Owen R., 1854. Descriptive Catalogue of the Fossil Organic Remains of Reptilia and Pisces Contained in the Museum of the Royal College of Surgeons of England, p. 184. Taylor and Francis, London.
180. Padian, K., 2013. The problem of dinosaur origins: integrating three approaches to the rise of Dinosauria. *Earth and Environmental Science Transactions of the Royal Society of Edinburgh*, *103*(3-4), pp.423–442. https://doi.org/10.1017/S1755691013000431
181. Pankhurst, R.J., Rapela, C.W., Fanning, C.M. and Márquez, M., 2006. Gondwanide continental collision and the origin of Patagonia. *Earth-Science Reviews*, *76*(3-4), pp.235–257.
182. Pankhurst, R.J., Rapela, C.W., De Luchi, M.L., Rapalini, A.E., Fanning, C.M. and Galindo, C., 2014. The Gondwana connections of northern Patagonia. *Journal of the Geological Society*, *171*(3), pp.313–328.
183. Porro, L.B., Butler, R.J., Barrett, P.M., Moore-Fay, S. and Abel, R.L., 2010. New heterodontosaurid specimens from the Lower Jurassic of southern Africa and the early ornithischian dinosaur radiation. *Earth and Environmental Science Transactions of the Royal Society of Edinburgh*, *101*(3-4), pp.351–366. doi:10.1017/S175569101102010X.
184. Porro, L.B., Witmer, L.M. and Barrett, P.M., 2015. Digital preparation and osteology of the skull of *Lesothosaurus diagnosticus* (Ornithischia: Dinosauria). *PeerJ*, *3*, p.e1494.
185. Raath, M.A., 1969. A new coelurosaurian dinosaur from the Forest Sandstone of Rhodesia. *Arnoldia, 4*(28), pp.1–25.
186. Raath, M.A., 1981. A protosuchid crocodilian from the Forest Sandstone Formation (upper Karoo) of Zimbabwe. *Palaeontologia africana 24*, pp.69–174.
187. Raath, M.A., Kitching, J.W., Shone, R.W. and Rossouw, G.J., 1990. Dinosaur tracks in Triassic Molteno sediments: the earliest evidence of dinosaurs in South Africa? *Palaeontologia africana 27*, pp.89–95.
188. Raath, M.A., Smith, C.C. and Bond, G., 1970. A new Upper Karroo dinosaur fossil locality on the lower Angwa River, Sipolilo District, Rhodesia. *Arnoldia, 4*(35), pp.1–10.
189. Rademan, Z., 2018. *Radiometric dating and stratigraphic reassessment of the Elliot and Clarens formations; near Maphutseng and Moyeni, Kingdom of Lesotho, southern Africa*. (MSc thesis, Stellenbosch University). http://hdl.handle.net/10019.1/104888
190. Rainforth, E.C., 2003. Revision and re–evaluation of the Early Jurassic dinosaurian ichnogenus *Otozoum*. *Palaeontology 46*, pp.803–838.
191. Ramezani, J., Fastovsky, D.E. and Bowring, S.A., 2014. Revised chronostratigraphy of the lower Chinle Formation strata in Arizona and New Mexico (USA): high-precision U-Pb geochronological constraints on the Late Triassic evolution of dinosaurs. *American Journal of Science*, *314*(6), pp.981–1008.
192. Ramezani, J., Hoke, G.D., Fastovsky, D.E., Bowring, S.A., Therrien, F., Dworkin, S.I., Atchley, S.C. and Nordt, L.C., 2011. High-precision U-Pb zircon geochronology of the Late Triassic Chinle Formation, Petrified Forest National Park (Arizona, USA): Temporal constraints on the early evolution of dinosaurs. *Bulletin*, *123*(11-12), pp.2142–2159.
193. Rampersadh, A., Bordy, E.M., Sciscio, L. and Abrahams, M., 2018. Dinosaur behaviour in an Early Jurassic palaeoecosystem–uppermost Elliot Formation, Ha Nohana, Lesotho. *Annales Societatis Geologorum Poloniae*, *88*(2), pp.163–179.
194. Raup, D.M. and Sepkoski, J.J., 1982. Mass extinctions in the marine fossil record. *Science*, *215*(4539), pp.1501–1503.

195. Raven, T.J., Barrett, P.M., Xu, X. and Maidment, S.C.R., 2019. A reassessment of the purported ankylosaurian dinosaur *Bienosaurus lufengensis* from the Lower Lufeng Formation of Yunnan, People's Republic of China. *Acta Palaeontologia Polonica*, *64*, pp.335–342. doi:10.4202/app.00577.2018
196. Ray, S. and Chinsamy, A., 2002. A theropod tooth from the Late Triassic of southern Africa. *Journal of Biosciences*, 27(3), pp.295–298.
197. Rayfield, E.J., Barrett, P.M. and Milner, A.R., 2009. Utility and validity of Middle and Late Triassic 'land vertebrate faunachrons'. *Journal of Vertebrate Paleontology*, *29*(1), pp.80–87.
198. Rogers, R.R., Rogers, K.C., Munyikwa, D., Terry, R.C. and Singer, B.S., 2004. Sedimentology and taphonomy of the upper Karoo-equivalent Mpandi Formation in the Tuli Basin of Zimbabwe, with a new 40Ar/39Ar age for the Tuli basalts. *Journal of African Earth Sciences*, *40*(3-4), pp.147–161.
199. Rossignol, C., Hallot, E., Bourquin, S., Poujol, M., Jolivet, M., Pellenard, P., Ducassou, C., Nalpas, T., Heilbronn, G., Yu, J. and Dabard, M.P., 2019. Using volcaniclastic rocks to constrain sedimentation ages: To what extent are volcanism and sedimentation synchronous?. *Sedimentary geology*, *381*, pp.46–64. https://doi.org/10.1016/j.sedgeo.2018.12.010.
200. Rowe, T. 1989. A new species of the theropod dinosaur *Syntarsus* from the Early Jurassic Kayenta Formation of Arizona. *Journal of Vertebrate Palaeontology*, *9*, 125-136.
201. Rubidge, B.S., Erwin, D.H., Ramezani, J., Bowring, S.A. and de Klerk, W.J., 2013. High-precision temporal calibration of Late Permian vertebrate biostratigraphy: U-Pb zircon constraints from the Karoo Supergroup, South Africa. *Geology*, *41*(3), pp.363–366.
202. Schiuma, M. and Llambias, E.J., 2008. New ages and chemical analysis on Lower Jurassic volcanism close to the dorsal de Huincul, Neuquen. *Revista de la Asociación Geológica Argentina*, *63*, pp.644–652.
203. Sciscio, L. and Bordy, E.M., 2016. Palaeoclimatic conditions in the Late Triassic-Early Jurassic of southern Africa: a geochemical assessment of the Elliot Formation. *Journal of African Earth Sciences*, *119*, pp.102–119.
204. Sciscio, L., Bordy, E.M., Abrahams, M., Knoll, F., McPhee, B.W., 2017b. The first megatheropod tracks from the Lower Jurassic upper Elliot Formation, Karoo Basin, Lesotho. PLOS One 12(10): e0185941. https://doi.org/10.1371/journal.pone.0185941
205. Sciscio, L., 2016. *Position of the Triassic-Jurassic boundary in South Africa and Lesotho: A multidisciplinary approach aimed at improving the chronostratigraphy and biostratigraphy of the Elliot Formation, Stormberg Group* (Doctoral dissertation, University of Cape Town). http://hdl.handle.net/11427/20847.
206. Sciscio, L., Bordy, E.M., Reid, M. and Abrahams, M., 2016. Sedimentology and ichnology of the Mafube dinosaur track site (Lower Jurassic, eastern Free State, South Africa): a report on footprint preservation and palaeoenvironment. *PeerJ*, *4*, p.e2285.
207. Sciscio, L., de Kock, M., Bordy, E. and Knoll, F., 2017a. Magnetostratigraphy across the Triassic-Jurassic boundary in the main Karoo Basin. *Gondwana Research*, *51*, pp.177–192. doi:10.1016/j.gr.2017.07.009
208. Sciscio, L., Knoll, F., Bordy, E.M., de Kock, M.O. and Redelstorff, R., 2017c. Digital reconstruction of the mandible of an adult *Lesothosaurus diagnosticus* with insight into the tooth replacement process and diet. *PeerJ*, *5*, p.e3054.
209. Sell, B., Ovtcharova, M., Guex, J., Bartolini, A., Jourdan, F., Spangenberg, J.E., Vicente, J.C. and Schaltegger, U., 2014. Evaluating the temporal link between the Karoo LIP and climatic–biologic events of the Toarcian Stage with high-precision U–Pb geochronology. *Earth and Planetary Science Letters*, *408*, pp.48–56.
210. Sereno, P.C., 2012. Taxonomy, morphology, masticatory function and phylogeny of heterodontosaurid dinosaurs. *ZooKeys*, *226*, pp.1–225.
211. Shubin, N.H. and Sues, H.D., 1991. Biogeography of early Mesozoic continental tetrapods: patterns and implications. *Paleobiology*, *17*(3), pp.214–230.
212. Shubin, N.H., Crompton, A.W., Sues, H.D. and Olsen, P.E., 1991. New fossil evidence on the sister-group of mammals and early Mesozoic faunal distributions. *Science*, *251*(4997), pp.1063–1065. doi:10.1126/science.251.4997.1063. PMID:17802092.
213. Sidor, C.A. and Hancox, P.J., 2006. *Elliotherium kersteni*, a new tritheledontid from the lower Elliot Formation (Upper Triassic) of South Africa. *Journal of Paleontology*, *80*(2), pp.333–342.
214. Smith, R. and Kitching, J., 1997. Sedimentology and vertebrate taphonomy of the *Tritylodon* Acme Zone: a reworked palaeosol in the Lower Jurassic Elliot Formation, Karoo Supergroup, South Africa. *Palaeogeography, Palaeoclimatology, Palaeoecology*, *131*(1-2), pp.29–50.
215. Smith, R.M., Marsicano, C.A. and Wilson, J.A., 2009. Sedimentology and paleoecology of a diverse Early Jurassic tetrapod tracksite in Lesotho, southern Africa. *Palaios*, *24*(10), pp.672–684.

216. Smith, R.M.H., Eriksson, P.G. and Botha, W.J., 1993. A review of the stratigraphy and sedimentary environments of the Karoo-aged basins of Southern Africa. *Journal of African Earth Sciences*, *16*(1-2), pp.143–169.
217. Spencer, C.J., Kirkland, C.L. and Taylor, R.J., 2016. Strategies towards statistically robust interpretations of in situ U–Pb zircon geochronology. *Geoscience Frontiers, 7*, pp.581–589.
218. Spikings, R., Reitsma, M.J., Boekhout, F., Mišković, A., Ulianov, A., Chiaradia, M., Gerdes, A. and Schaltegger, U., 2016. Characterisation of Triassic rifting in Peru and implications for the early disassembly of western Pangaea. *Gondwana Research*, *35*, pp.124–143.
219. Suarez, C.A., Knobbe, T.K., Crowley, J.L., Kirkland, J.I. and Milner, A.R., 2017. A chronostratigraphic assessment of the Moenave Formation, USA using C-isotope chemostratigraphy and detrital zircon geochronology: Implications for the terrestrial end Triassic extinction. *Earth and Planetary Science Letters*, *475*, pp.83–93.
220. Sues, H.D. and Olsen, P.E., 2015. Stratigraphic and temporal context and faunal diversity of Permian-Jurassic continental tetrapod assemblages from the Fundy rift basin, eastern Canada. *Atlantic Geology, 51*, pp.139–205. doi:10.4138/atlgeol.2015.006.
221. Sues, H.D. and Reisz, R.R., 1995. First record of the early Mesozoic sphenodontian *Clevosaurus* (Lepidosauria: Rhynchocephalia) from the Southern Hemisphere. *Journal of Paleontology*, *69*(1), pp.123–126. doi:10.1017/s0022336000026974
222. Sues, H.D., Shubin, N.H., Olsen, P.E. and Amaral, W.W., 1996. On the cranial structure of a new protosuchid (Archosauria: Crocodyliformes) from the McCoy Brook Formation (Lower Jurassic) of Nova Scotia, Canada. *Journal of Vertebrate Paleontology*, *16*(1), pp.34–41. doi:10.1080/02724634.1996.10011281.
223. Svensen, H., Corfu, F., Polteau, S., Hammer, Ø. and Planke, S., 2012. Rapid magma emplacement in the Karoo large igneous province. *Earth and Planetary Science Letters*, *325*, pp.1–9. https://doi.org/10.1016/j.epsl.2012.01.015
224. Tauxe, L., 1998. Paleomagnetic Principles and Practice - Modern approaches in geophysics. Kluwer Academic Publisher, Dordrecht, Netherlands, pp.309.
225. Tabor, N.J. and Myers, T.S., 2015. Paleosols as indicators of paleoenvironment and paleoclimate. *Annual Review of Earth and Planetary Sciences, 43*, pp.333–361.
226. Thulborn, R.A., 1974. A new heterodontosaurid dinosaur (Reptilia: Ornithischia) from the Upper Triassic Red Beds of Lesotho. *Zoological Journal of the Linnean Society of Londo*n *55*, pp.151–175.
227. Tolchard, F., Nesbitt, S.J., Desojo, J., Viglietti, P., Butler, R.J. and Choiniere, J.N., 2019. 'Rauisuchian' material from the lower Elliot Formation of South Africa: implications for Late Triassic biogeography and biostratigraphy. *Journal of African Earth Sciences*, *160,* p.103610.
228. Tucker, R.T., Roberts, E.M., Hu, Y., Kemp, A.I. and Salisbury, S.W., 2013. Detrital zircon age constraints for the Winton Formation, Queensland: contextualizing Australia's Late Cretaceous dinosaur faunas. *Gondwana Research*, *24*(2), pp.767–779. http://dx.doi.org/10.1016/j.gr.2012.12.009.
229. Van Hoepen, E.C.N., 1920. Contributions to the knowledge of the reptiles of the Karoo Formation. 6. Further dinosaurian material in the Transvaal Museum. *Annals of the Transvaal Museum* 7, pp.93–140.
230. Viglietti, P.A., Frei, D., Rubidge, B.S. and Smith, R.M., 2018a. U-Pb detrital zircon dates and provenance data from the Beaufort Group (Karoo Supergroup) reflect sedimentary recycling and air-fall tuff deposition in the Permo-Triassic Karoo foreland basin. *Journal of African Earth Sciences*, *143*, pp.59–66.
231. Viglietti, P.A., Barrett, P.M., Broderick, T.J., Munyikwa, D., MacNiven, R., Broderick, L., Chapelle, K., Glynn, D., Edwards, S., Zondo, M., Broderick, P. and Choiniere, J.N., 2018b. Stratigraphy of the *Vulcanodon* type locality and its implications for regional correlations within the Karoo Supergroup. *Journal of African Earth Sciences*, *137*, pp.149–156. doi: 10.1016/j.jafrearsci.2017.10.015
232. Viglietti, P.A., McPhee, B.W., Bordy, E.M., Sciscio, L., Barrett, P.M., Benson, R.B., Wills, S., Tolchard, F. and Choiniere, J.N., in press a. Biostratigraphy of the *Scalenodontoides* Assemblage Zone (Stormberg Group, Karoo Supergroup), South Africa. *South African Journal of Geology.*
233. Viglietti, P.A., McPhee, B.W., Bordy, E.M., Sciscio, L., Barrett, P.M., Benson, R.B., Wills, S., Chapelle, K.J.E., Dollman, K.N., Mdekazi, C. and Choiniere, J.N., in press b. Biostratigraphy of the *Massospondylus* Assemblage Zone (Stormberg Group, Karoo Supergroup), South Africa. *South African Journal of Geology*.
234. Visser, J.N.J., 1984. A review of the Stormberg Group and Drakensberg volcanics in southern Africa. *Palaeontologia africana, 25,* pp.5–27.
235. Wang, S., Stiegler, J., Amiot, R., Wang, X., Du, G.H., Clark, J.M. and Xu, X., 2017. Extreme ontogenetic changes in a ceratosaurian theropod. *Current Biology*, *27*(1), pp.144–148. doi:10.1016/j.cub.2016.10.043

236. Wang, Z.S., Rasbury, E.T., Hanson, G.N. and Meyers, W.J., 1998. Using the U-Pb system of calcretes to date the time of sedimentation of clastic sedimentary rocks. *Geochimica et Cosmochimica Acta, 62*(16), pp.2823–2835.
237. Warren, A. and Damiani, R., 1999. Stereospondyl amphibians from the Elliot Formation of South Africa. *Palaeontologia africana, 35,* pp.45–54. http://hdl.handle.net/10539/1646.
238. Whiteside, J.H., Olsen, P.E., Eglinton, T., Brookfield, M.E. and Sambrotto, R.N., 2011. Compound-specific carbon isotopes from EarthTs largest flood basalt eruptions directly linked to the end-Triassic mass extinction. *PNAS*, *107*(15), 6721–6725. https://doi.org/10.1073/pnas.1001706107.
239. Wilson, J.A., Marsicano, C.A. and Smith, R.M., 2009. Dynamic locomotor capabilities revealed by early dinosaur trackmakers from Southern Africa. *PLoS One*, *4*(10), p.e7331.
240. Wotzlaw, J.F., Guex, J., Bartolini, A., Gallet, Y., Krystyn, L., McRoberts, C.A., Taylor, D., Schoene, B. and Schaltegger, U., 2014. Towards accurate numerical calibration of the Late Triassic: High-precision U-Pb geochronology constraints on the duration of the Rhaetian. *Geology*, *42*(7), pp.571–574. doi: 10.1130/G35612.1.
241. Wu, Y. and Zheng, Y., 2004. Genesis of zircon and its constraints on interpretation of U-Pb age. *Chinese Science Bulletin*, *49*(15), pp.1554–1569.
242. Yates, A.M., 2003. A definite prosauropod dinosaur from the lower Elliot Formation (Norian: Upper Triassic) of South Africa. *Palaeontologia africana, 39*, pp.63–68.
243. Yates, A.M., 2005. A new theropod dinosaur from the Early Jurassic of South Africa and its implications for the early evolution of theropods. *Palaeontologia africana,* 41, pp.105–122.
244. Yates, A.M., 2007a. Solving a dinosaurian puzzle: the identity of *Aliwalia rex* Galton. *Historical Biology, 19*, pp.93–123.
245. Yates, A.M., 2007b. The first complete skull of the Triassic dinosaur *Melanorosaurus* Haughton (Sauropodomorpha: Anchisauria). *Special Papers in Paleontology, 77*, pp.9–55.
246. Yates, A.M., 2008. A second specimen of *Blikanasaurus* (Dinosauria: Sauropoda) and the biostratigraphy of the lower Elliot Formation. *Palaeontologia africana, 43*, pp.39–43.
247. Yates, A.M. and Barrett, P.M., 2010. *Massospondylus carinatus* Owen 1854 (Dinosauria: Sauropodomorpha) from the Lower Jurassic of South Africa: Proposed conservation of the usage by designation of a neotype. *Palaeontologia africana*, *45*, pp.7–10.
248. Yates, A.M., Bonnan, M.F., and Neveling, J., 2011. A new basal sauropodomorph dinosaur from the Early Jurassic of South Africa. *Journal of Vertebrate Paleontology, 31*, pp.610–625.
249. Yates, A.M., Bonnan, M.F., Neveling, J., Chinsamy, A. and Blackbeard, M.G., 2009. A new transitional sauropodomorph dinosaur from the Early Jurassic of South Africa and the evolution of sauropod feeding and quadrupedalism. *Proceedings of the Royal Society B: Biological Sciences*, *277*(1682), pp.787–794.
250. Yates, A.M. and Kitching, J.W., 2003. The earliest known sauropod dinosaur and the first steps towards sauropod locomotion. *Proceedings of the Royal Society of London. Series B: Biological Sciences*, *270*(1525), pp.1753–1758.
251. You, H.-L., Azuma, Y., Wang, T., Wang, Y.-M. and Don, Z.-M. 2014. The first well-preserved coelophysoid theropod dinosaur from Asia. *Zootaxa*, *3873*, 233–249.
252. Zeigler, K.E. and Geissman, J.W., 2011. Magnetostratigraphy of the Upper Triassic Chinle Group of New Mexico: Implications for regional and global correlations among Upper Triassic sequences. *Geosphere*, *7*(3), pp.802–829.